Trust & Quality

Inspecta

INSPECTA

TECHNICAL REPORT

SKB

Damage tolerance analysis of BWR-canister inserts for spent nuclear fuel in the case of an earthquake induced rock shear load – Influence of using more detailed models

Report No.: 5000264-1

Revision No.: 2

INSPECTA TECHNOLOGY AB

BOX 30100 104 25 STOCKHOLM SWEDEN TEL (+46) 8 5011 3000 FAX (+46) 8 5011 3001 www.inspecta.com

Date	Our project No.
2015-01-29	5000264
Approved by	Organizational unit
Keivan Ashhami	Inspecta Technology AB
Customer	Customer reference
SKB	Mikael Jonsson

Summary

In this report, a comparison is made between the original model of the BWR insert (using a simplified idealization of the geometry) and a more advanced model where the channel tubes are not tied to the insert and the support plates are modelled separately from the insert. Also, the impact of manufacturing tolerances is evaluated, where the steel tube cassette is shifted so that it is closer to the outside of the insert (i.e. a decreased edge distance).

The comparison shows that all the new models have locally higher stresses compared to the original model. The reason for these high stresses is mainly dependent on the element meshes, which are not designed to be used in a damage tolerance analysis. For example, many stress concentrations is directly related to the use of wedge elements. In all cases, disregarding the elements that behaves poorly significantly reduces the locally higher tensile stresses. There are also regions with slightly elevated stress concentrations, but they are of minor importance because the neighbouring elements have significantly lower stresses.

Both the original model and all the new models have axial stresses of the same magnitude in the most important region for the damage tolerance analysis. This shows that it is not necessary to perform a completely renewed damage tolerance analysis at more positions in the insert or at the location with the smallest distance between the channel tubes and the outside of the insert.

Report title	
Damage tolerance analysis of BWR-canister inserts for spent nuclear fuel in the case of an earthquake induced rock shear load – Influence of using more detailed models	Index terms
Work carried out by	Distribution
Peter Dillström	☒ No distribution without permission from the customer or Inspecta Technology AB.
Work verified by	☐ Limited internal distribution in Inspecta Technology AB.
Lars Alverlind	☐ Unrestricted distribution.

Table of content ***Page***

1 INTRODUCTION

SKB has conducted many analyses of the canister insert, which is summarized in the design analysis [1]. When SSM reviewed these analyses [2] they emphasised a need for a number of more detailed analyses of the shear load case. Among other things, SSM wanted that SKB should evaluate the following:

- Impact of the assumption that the steel channel tubes were tied to the insert.
- The manufacturing tolerance of the distance between the channel tubes and insert outer surface and what effect it has on the mechanical integrity.

To answer the above questions, SKB has conducted new analyses [3] which, among other things, evaluate the impact of the aspects listed below:

- In the previous analysis [4] it was assumed that the channel tubes were "welded together" with the rest of the insert. The new analysis assumed that the channel tubes are not bonded to the insert and therefore the contact condition between channel tubes and the insert is now part of the analysis.
- The channel tubes are welded to support plates in order to create the steel tube cassette. In the previous analysis, the support plates were not modelled, instead they were considered as a part of the insert. In the new analysis, the support plates are modelled separately from the nodular cast iron insert.
- In the previous analysis it was assumed that the steel tube cassette was centered in the insert. In the new analysis the impact of manufacturing tolerances are evaluated, where the steel tube cassette is shifted so that it is closer to the outside of the insert (i.e. a decreased edge distance H in Fig. 1-1).

The conclusion from the new analysis [3] is that the results show rather small differences compared to the previous analysis [4] that was based on a much more simplified geometry.

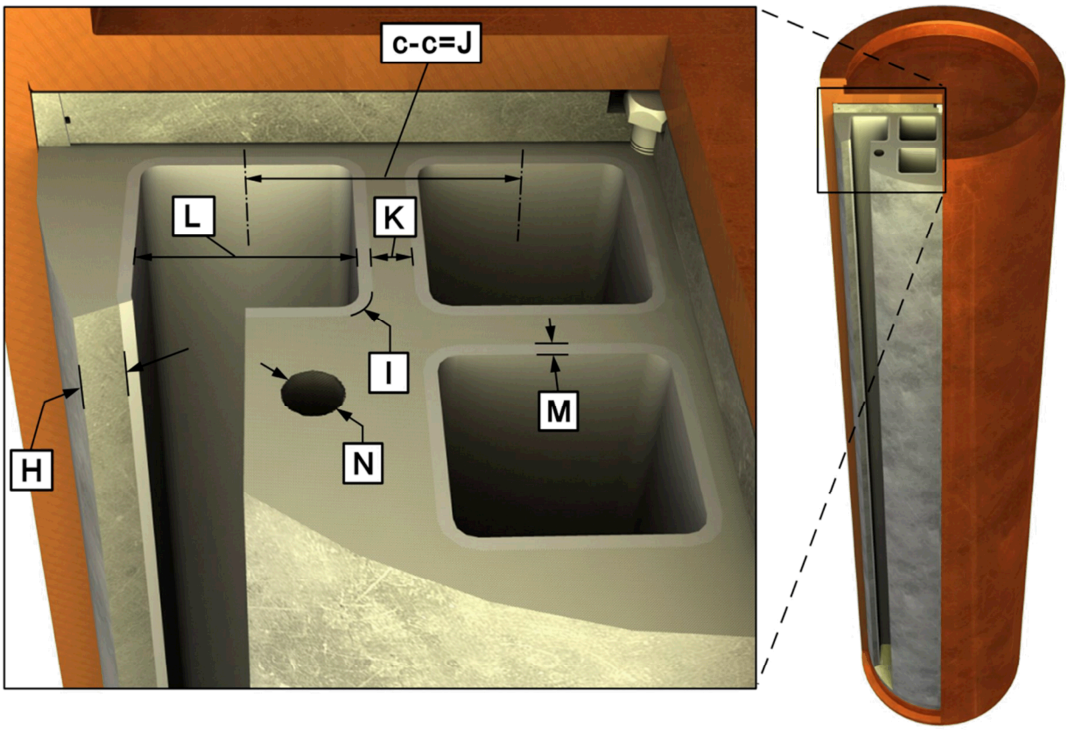

Figure 1-1. The insert with channel tubes, the edge distance H is decreased in the new analysis.

SSM has reviewed the new analyses [5] and would like SKB to clarify the following issues:

- SSM question 2.

  In the new analyses, SKB reports locally higher stresses as compared with the earlier analyses (also in new positions). SSM believes that this means that SKB needs to identify the minimum acceptable defect size at more positions than in the earlier analyses (both in the axial direction and in different parts of a specific cross-section).

- SSM question 3.

  SKB has conducted the analyses so that the minimum distance between the edge of the channel tubes and the insert surface is where you have high compressive stresses. SSM considers it more appropriate to carry out the analysis so as to have high tensile stresses in this area. Moreover SSM wants a new assessment of what this means for the damage tolerance of the insert.

SKB has therefore revised the new analyses to ensure that tensile stresses are obtained in the area with the smallest distance between the edge of the channel tubes and the insert surface. Furthermore, in the revised analyses [6], correct manufacturing tolerances regarding the steel tube cassette shift are introduced (i.e. that an off-set of the steel tube cassette of 10 mm is acceptable [8]).

The purpose of this report is to perform an evaluation on the necessity of a completely renewed damage tolerance analysis. This evaluation will concentrate on the issues raised by SSM [5] (i.e. SSM question 2-3).

2 SUMMARY OF THE ORIGINAL DAMAGE TOLERANCE ANALYSIS

The original damage tolerance analysis is given in [7] using the data from the original global model presented in [4]. In this report we are only interested in the worst case presented in [4, 7] which is going to be compared with the revised global analysis presented in [6]. This means that the following assumptions are used in the evaluation:

- A horizontal shear plane at ¾-distance from the insert base, which is identified as the most severe shear plane position for the insert according to previous studies [6].
- A rock shear = 5 cm shear movement at a velocity of 1 m/s.
- The buffer has a density of 2050 kg/m^3 (Ca-bentonite).
- A postulated semi-elliptical surface crack (length/depth = 6).

The global model for the original analysis, using a more simplified geometry, is called model6g_normal_quarter_2050ca3 [4, 7].

2.1 Results from the original damage tolerance analysis

For the design case, bentonite density = 2050 kg/m^3 and shear = 5 cm, the acceptable defect depth = 4.5 mm and the acceptable defect length = 27.0 mm (using the most severe defect geometry assumption of a postulated semi-elliptical surface crack). Other defect geometry assumptions, defect locations and defect orientations give larger acceptable defect sizes.

2.2 Results from the original global model (model6g_normal_quarter_2050ca3)

For this model the maximum principal stress (333.3 MPa) is equal to the maximum stress in the axial direction of the insert (S33 = 333.2 MPa, see Fig. 2-1). This shows that there are no locally higher stresses in other areas for this model. The position of the maximum tensile stresses is also the position where the postulated semi-elliptical surface crack is analysed (see Fig. 2-2 and 2-3).

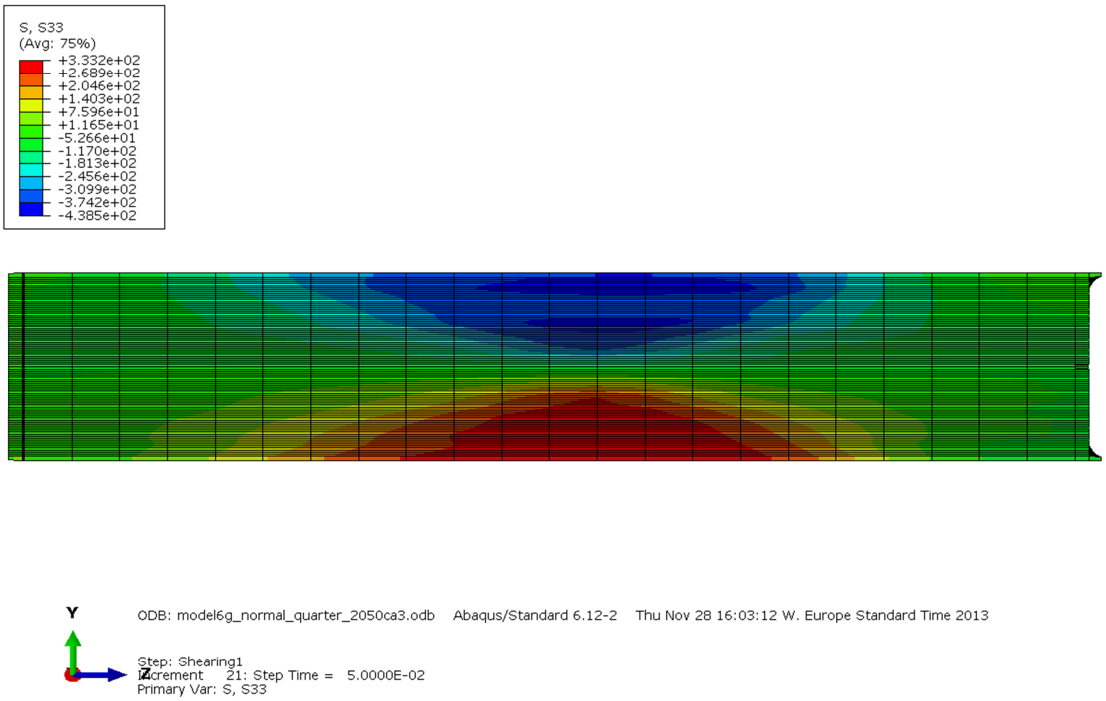

Figure 2-1. The maximum stress in the axial direction (S33) for the model model6g_normal_quarter_2050ca3 (plot of the entire insert).

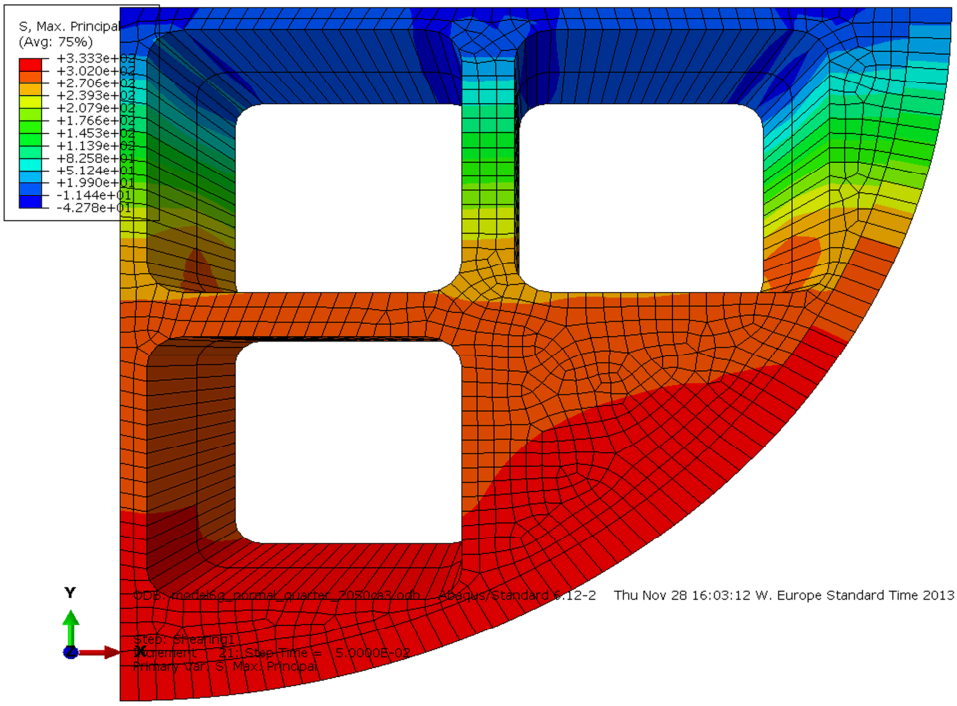

Figure 2-2. The maximum principal stress for the model model6g_normal_quarter_2050ca3.

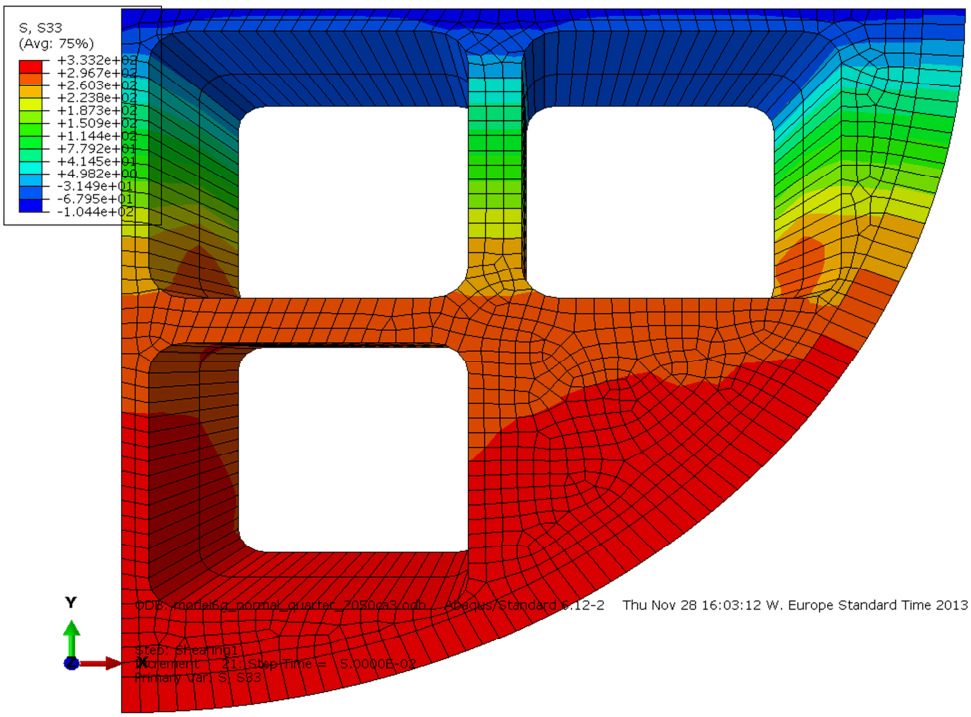

Figure 2-3. The maximum stress in the axial direction (S33) for the model model6g_normal_quarter_2050ca3.

However, there are problems with some of the elements and this is clear if you plot the above with 0% averaging between elements (see Fig. 2-4).

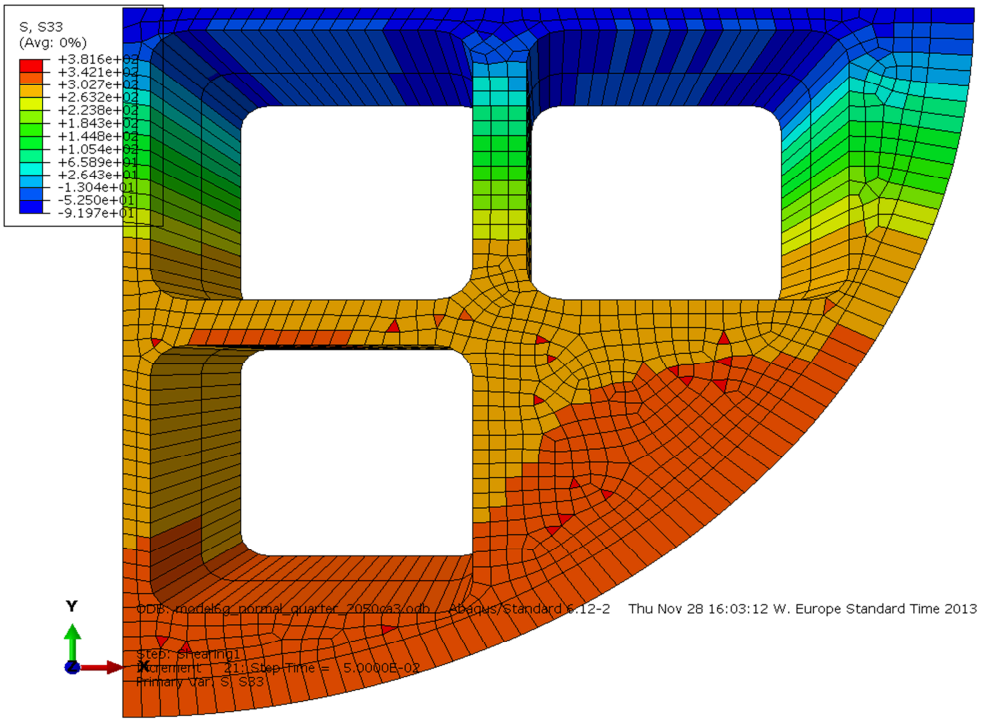

Figure 2-4. The maximum stress in the axial direction (S33) for the model model6g_normal_quarter_2050ca3 using 0% averaging between elements.

These locally higher stresses (382 MPa instead of 333 MPa) have nothing to do with the selected idealization but are mainly due to the poor behaviour of some elements (wedge elements, which is commonly used to get a mesh for a complex geometry). Also, it will have no impact on the damage tolerance analysis. To show the poor behaviour more clearly, the axial stress is plotted along a path in Fig. 2-5. (the path definition is also found in Fig. 2-5).

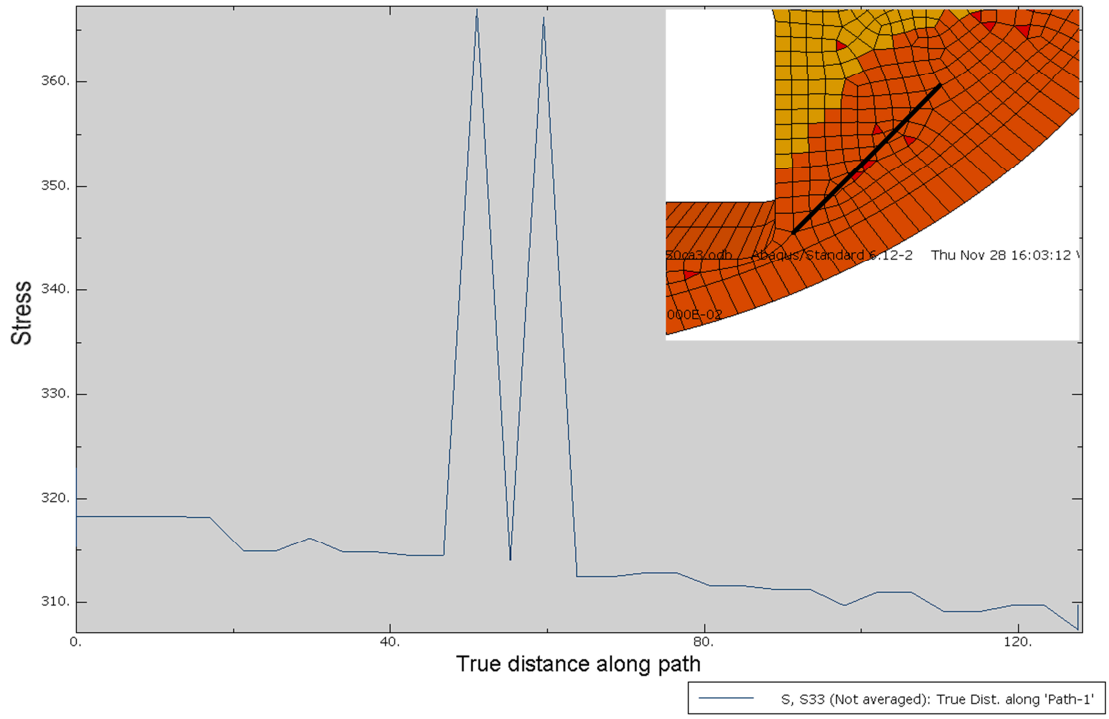

Figure 2-5. The stress in the axial direction (S33), along a given path, for the model model6g_normal_quarter_2050ca3 using 0% averaging between elements.

As shown in Fig. 2-5, the wedge elements behave poorly even though the stress field in this part of the model is almost constant. This poor behaviour for the wedge elements will be more extreme if the elements are located in a non-constant stress field or at a location with a stress concentration (the error in stress could be larger than 100-200%). This will be the case for all the revised global models examined in Sect. 3, 4 and 5. Since the elements adjacent to the wedge elements often are well behaved (if not another wedge element), disregarding the wedge element from the stress field will be a better approximation of the expected stress field (as shown in Fig. 2-5).

Finally, to simplify the comparison with the new more detailed models, a plot of the axial stress in the most important region for the damage tolerance analysis is given in Fig. 2-6. This axial stress is equivalent to an acceptable defect size = 4.5 mm [7] (defect length/depth = 6).

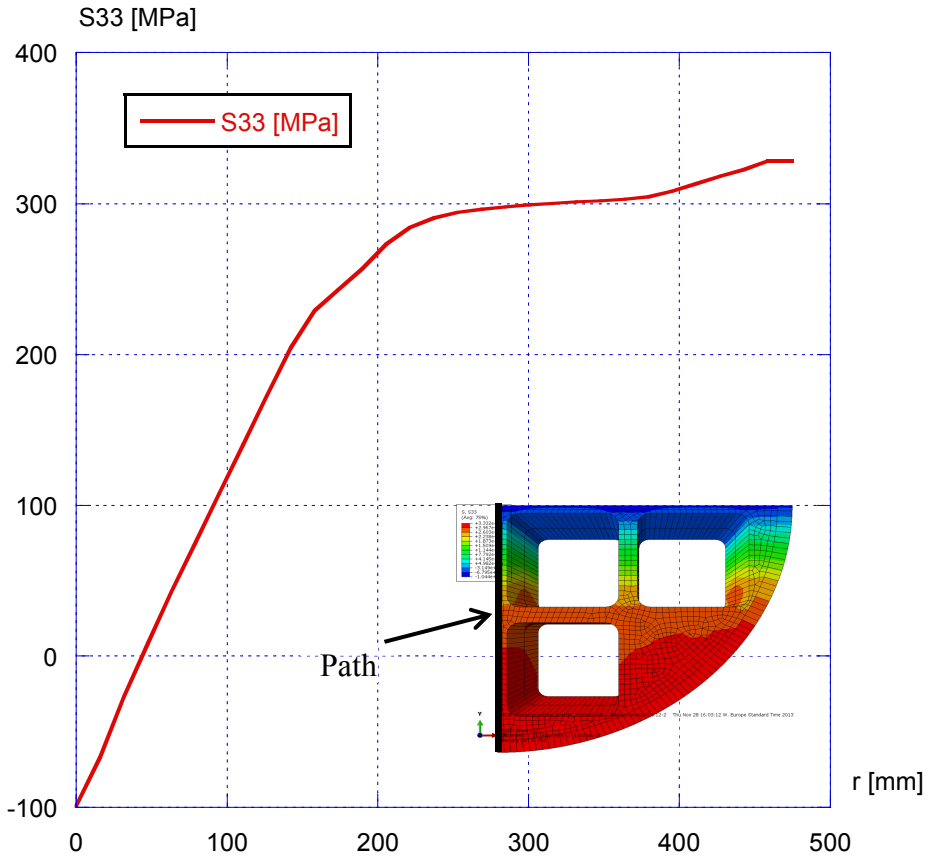

Figure 2-6. A path plot of the stress in the axial direction (S33) for the model model6g_normal_quarter_2050ca3 (the used path is given as a black line).

The axial stress, given in Fig. 2-6, could be compared with two shear load cases using smaller elastic bending loads where a simplified damage tolerance analysis could be done using ProSACC [9]. An estimate shows that an elastic bending load = 290 MPa is equivalent to an acceptable defect size = 18 mm and an elastic bending load = 200 MPa is equivalent to an acceptable defect size = 50 mm. This is summarised in Fig. 2-7.

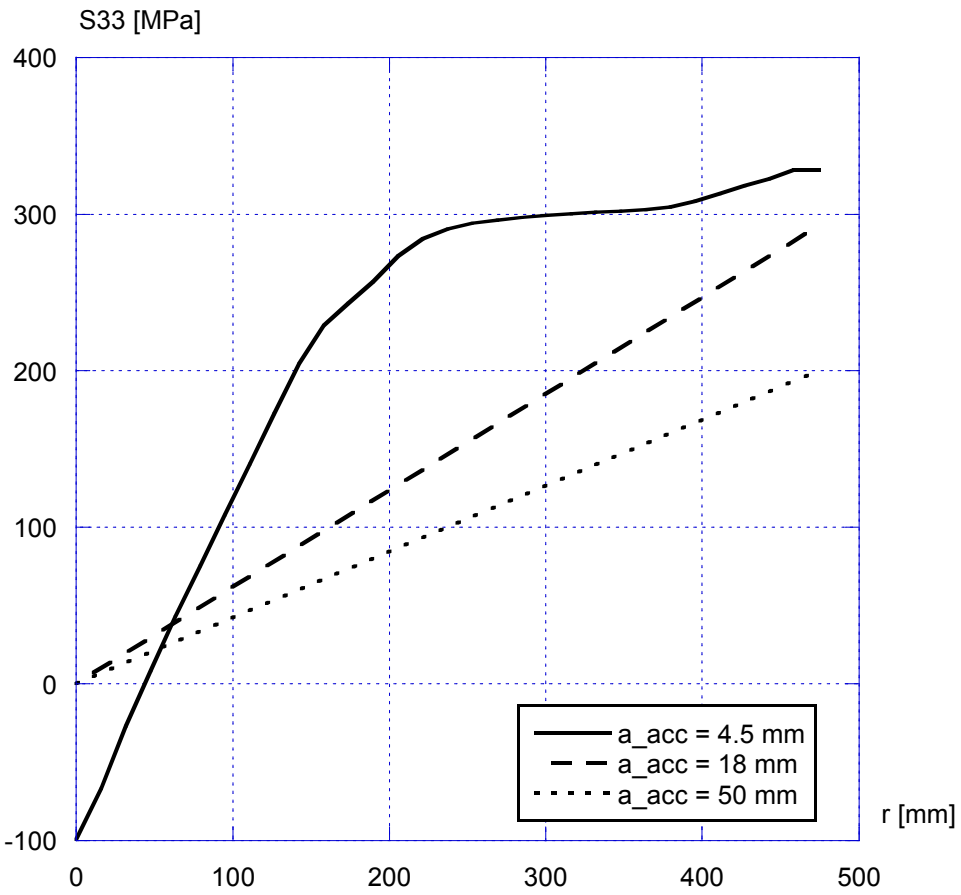

Figure 2-7. Path plots of the stress in the axial direction (S33) using different stress distributions (acceptable defect sizes are also given as a function of stresses).

The different stress distributions, as given in Fig. 2-7, are going to be used in the comparison with the different revised global analyses presented in [6].

3 RESULTS FROM THE REVISED GLOBAL MODEL (BWR_CENTRIC_ROTATED)

The revised global model bwr_centric_rotated is an idealization using a full model, where the steel tube cassette was centered in the insert, but the insert is rotated to have a small distance between the channel corner and insert outer radius (at the position with large axial stresses). As given in section 1, the revised global model assumes that the channel tubes are not tied to the insert and therefore the contact problem between channel tubes and the insert is now part of the analysis. Also, the support plates are modelled separately from the insert. More details of the revised model are given in [6].

For this model the maximum principal stress is equal to 870 MPa and the maximum stress in the axial direction of the insert, S33, is equal to 475.8 MPa (see Fig. 3-1). This shows that there are higher stresses in some areas for this model.

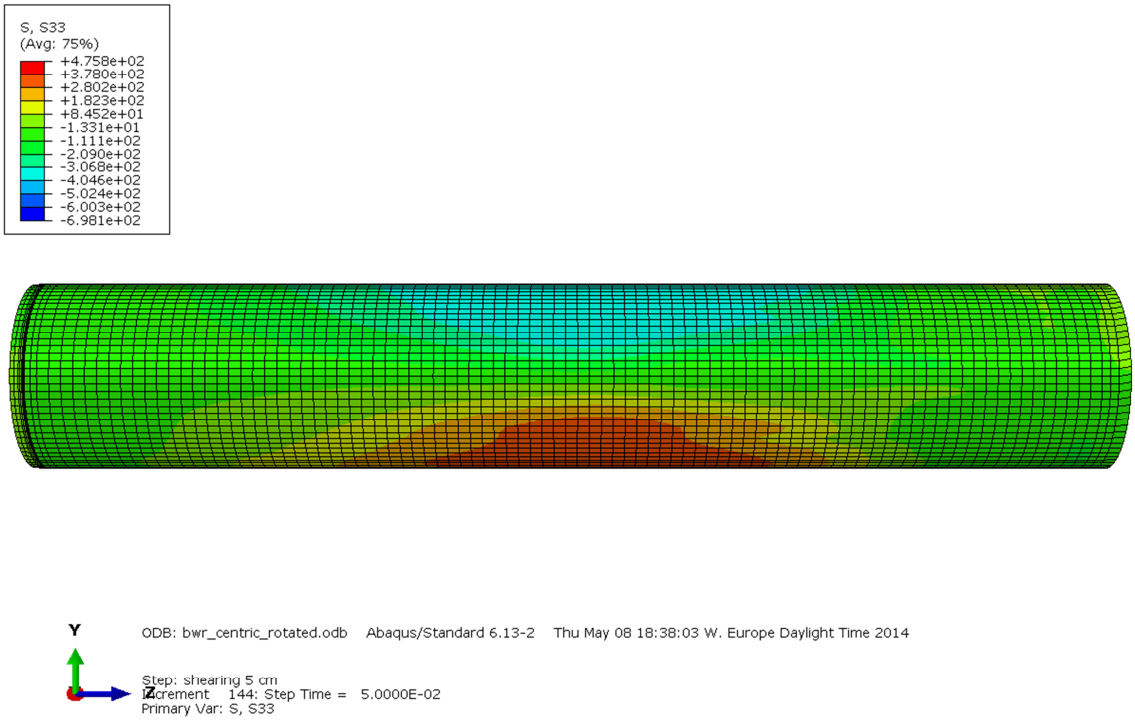

Figure 3-1. The maximum stress in the axial direction (S33) for the model bwr_centric_rotated (plot of the entire insert).

The stresses in the section where the maximum tensile stresses were located in the original analysis (see Sect. 2.2) are somewhat higher for this model. Both the maximum principal stress and the maximum stress in the axial direction of the insert, S33, are equal to 349.7 MPa (see Fig. 3-2). This means that the axial stresses are the most significant in this section, but that there are other areas of the insert that receives significantly higher tensile stresses.

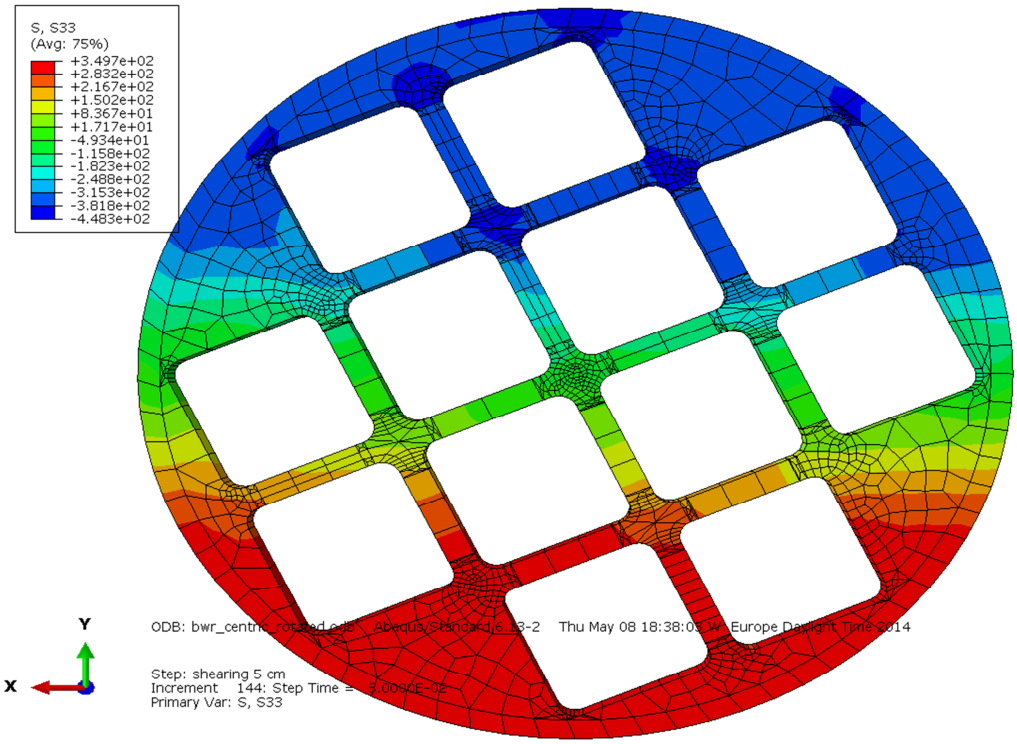

Figure 3-2. The stress in the axial direction (S33) for the model bwr_centric_rotated (at the section where the maximum tensile stresses were located in the original analysis). The prescribed shearing is acting in the y-direction.

Investigating the entire model, it is evident that the area with high tensile stresses (870 MPa) is located at the base of the insert (see Fig. 3-3).

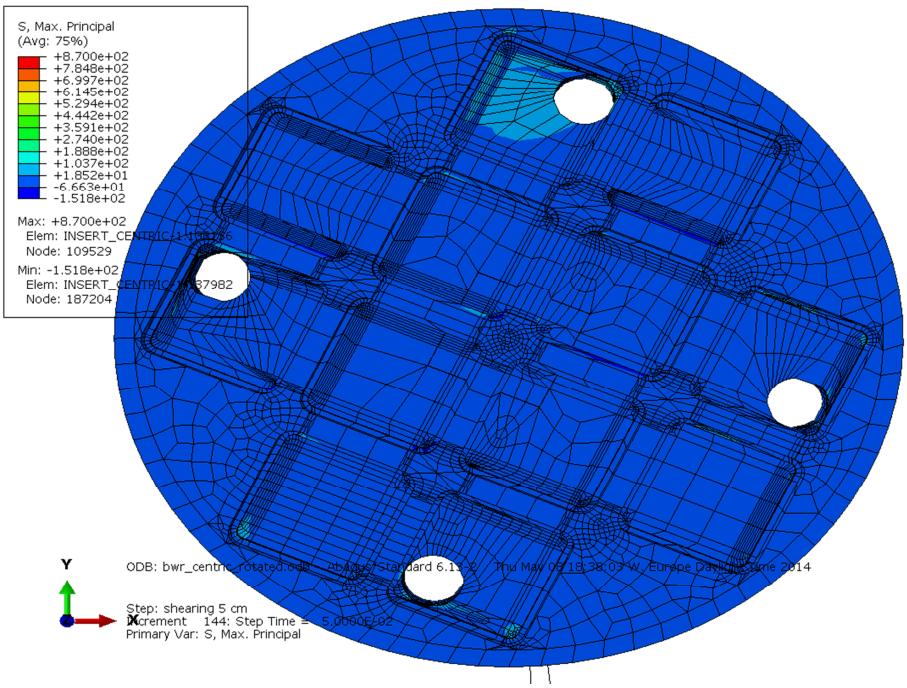

Figure 3-3. The maximum principal stress for the model bwr_centric_rotated (at the base of the insert). The screws are not part of the insert and are therefore not shown in this figure (i.e. the holes represent the positions of the screws).

When checking the base of the insert, it turns out that two elements inside the base part have a different behaviour that deviates from all other elements in the vicinity of this area (see Fig. 3-4).

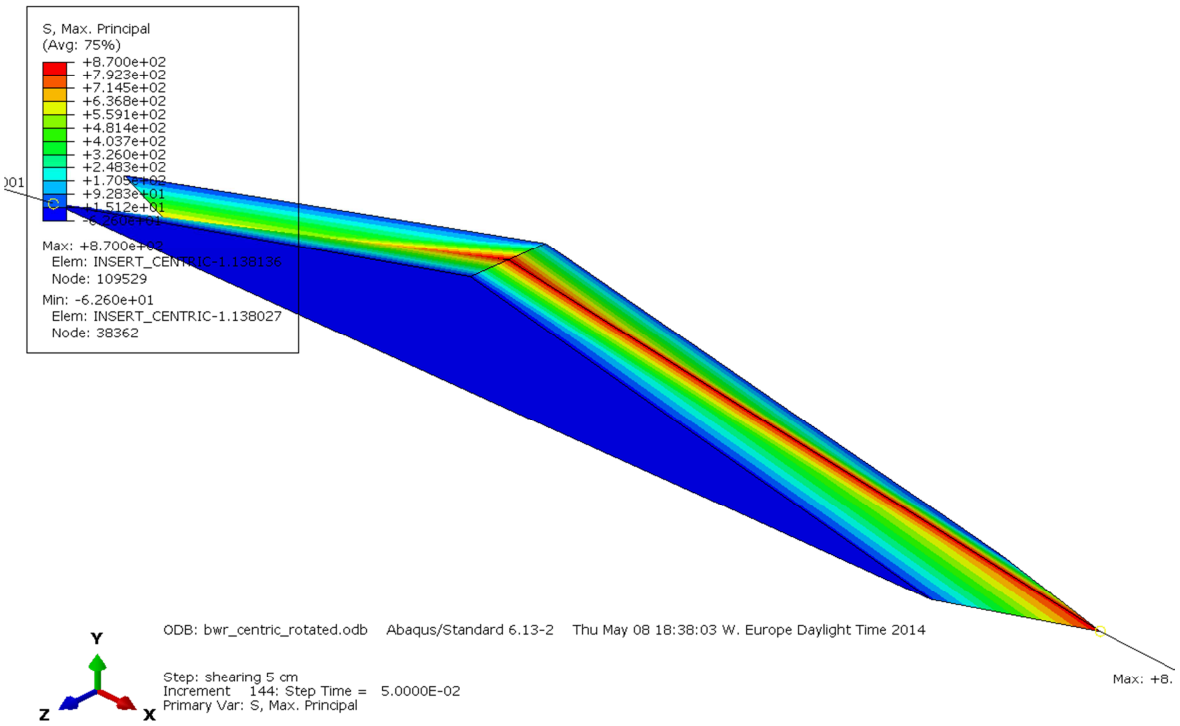

Figure 3-4. The maximum principal stress for the model bwr_centric_rotated (two elements inside the base part of the insert).

These two elements have no neighbouring elements with high stresses and it is obvious that these elements behave incorrectly and the results are not reliable. This can be verified by checking other stresses and strains in this part of the model (the effective plastic strain is 0.1%). To show the poor behaviour more clearly, the maximum principal stress is plotted along a path including neighbouring elements (see Fig. 3-5).

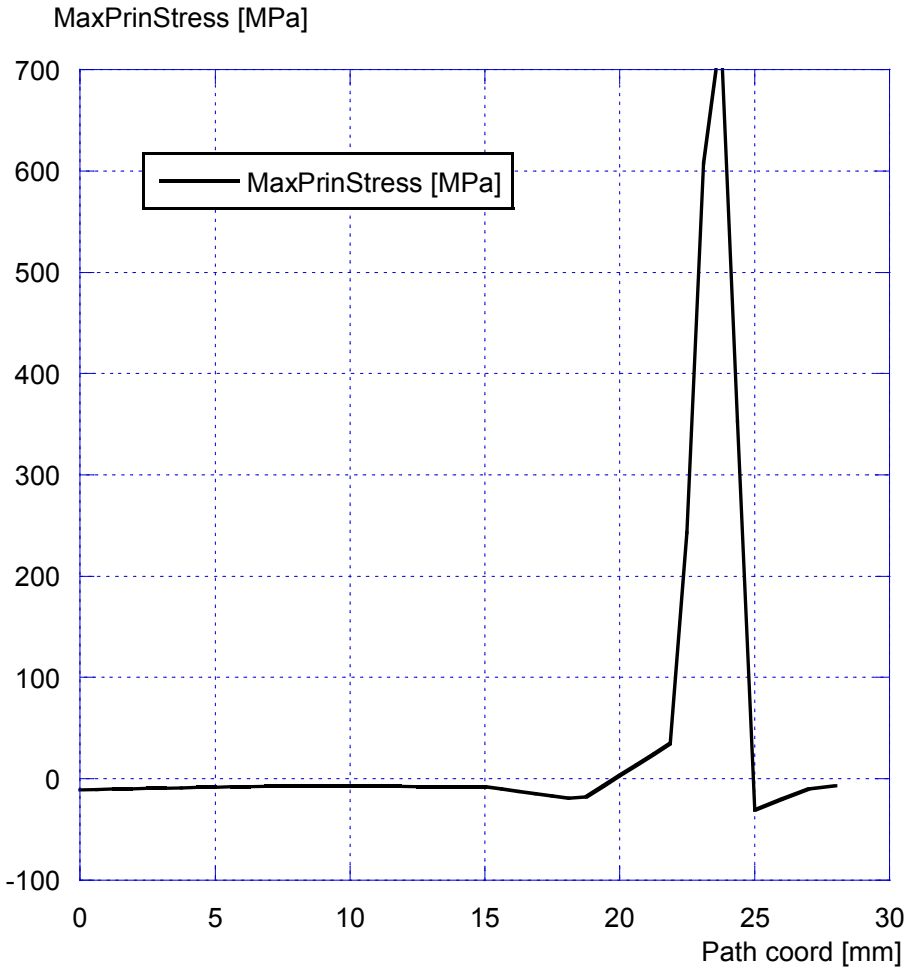

Figure 3-5. The maximum principal stress along a path including the elements that behave incorrectly and also the neighbouring elements (the base part of the insert).

As shown in Fig. 3-5, the maximum principal stress in the base part of the insert is generally in compression (as expected), except the two elements that behave incorrectly. These two elements should therefore be disregarded when performing a damage tolerance analysis.

If one removes the base part of the insert, the remaining part of the insert has a maximum principal stress equal to 377.1 MPa. This means that we still have a local tensile stress that is somewhat higher than in the original section as given in Fig. 3-2 (i.e. 349.7 MPa). Zooming into this area, one can see that this stress is concentrated in one element and it is adjacent to the now-modelled support plates that hold together the channel tubes (see Fig. 3-6).

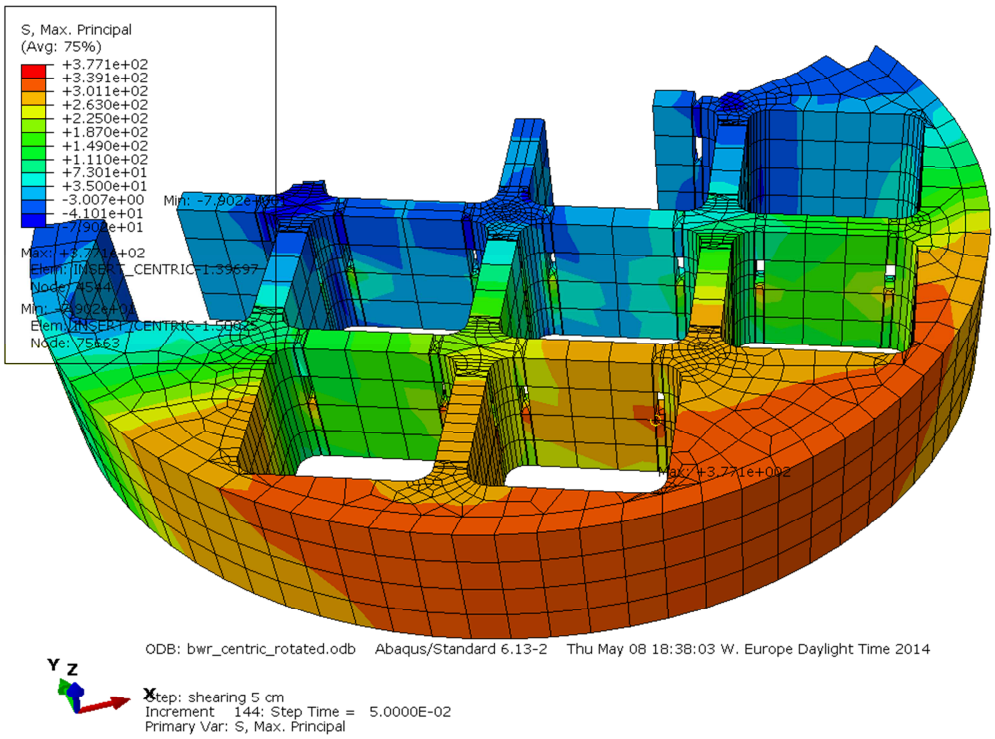

Figure 3-6. The maximum principal stress for the model bwr_centric_rotated (location with a local stress equal to 377.1 MPa).

The stress distribution along a path close to the stress concentration is then compared with the stresses given from the original damage tolerance analysis. This comparison is shown in Fig. 3-7.

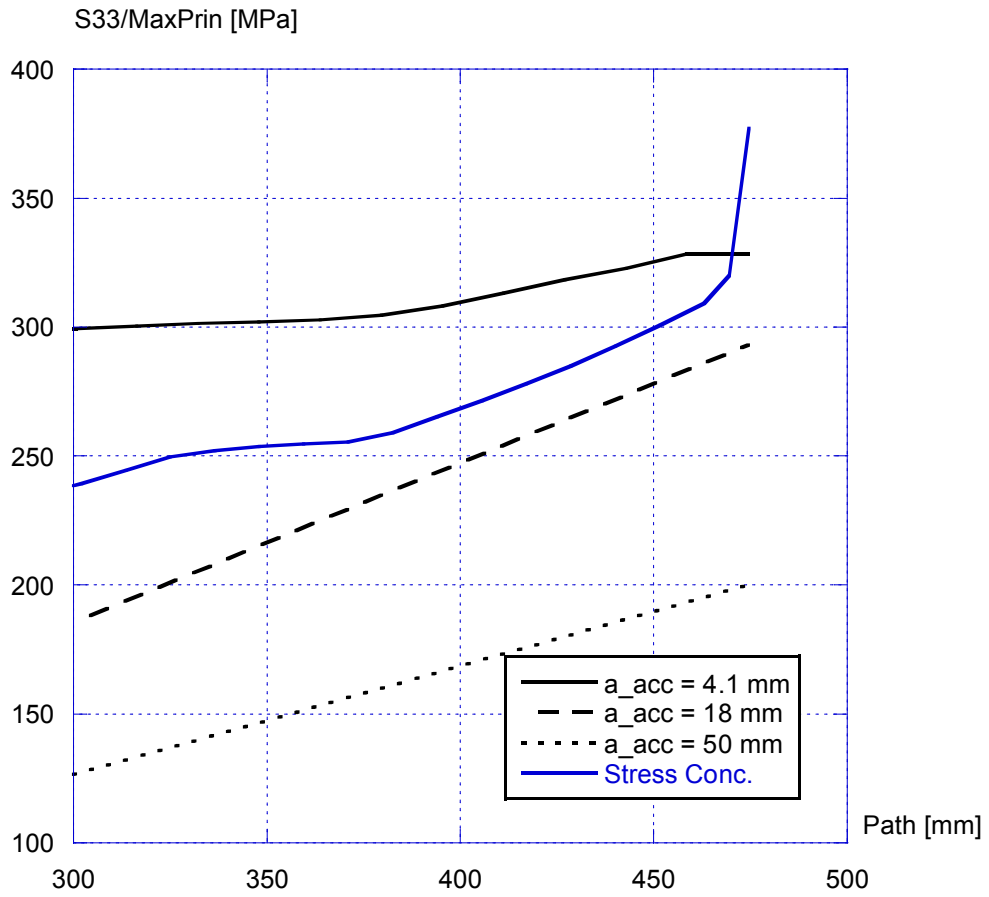

Figure 3-7. Comparison between the stresses close to the stress concentration and the stresses from the original damage analysis.

In a damage tolerance analysis, this slightly elevated stress concentration (within one element) can be neglected because the neighbouring elements have lower stresses and the width of the stress concentration is equal to the size of this element.

As given in Fig. 3-2, the stresses in the section where the maximum tensile stresses were located in the original analysis are somewhat higher for this model. The maximum stress in the axial direction of the insert, S33, are equal to 349.7 MPa (compared to 333.2 MPa from the original analysis). The region of higher axial stresses is magnified in Figure 3-8 to 3-9.

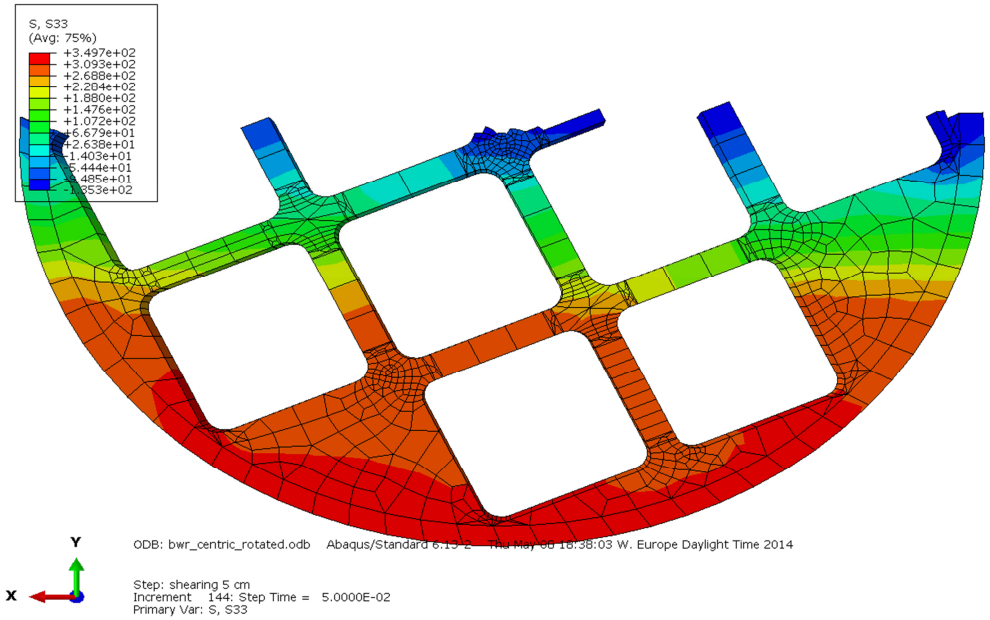

Figure 3-8. The stress in the axial direction (S33) for the model bwr_centric_rotated (at the section where the maximum tensile stresses were located in the original analysis).

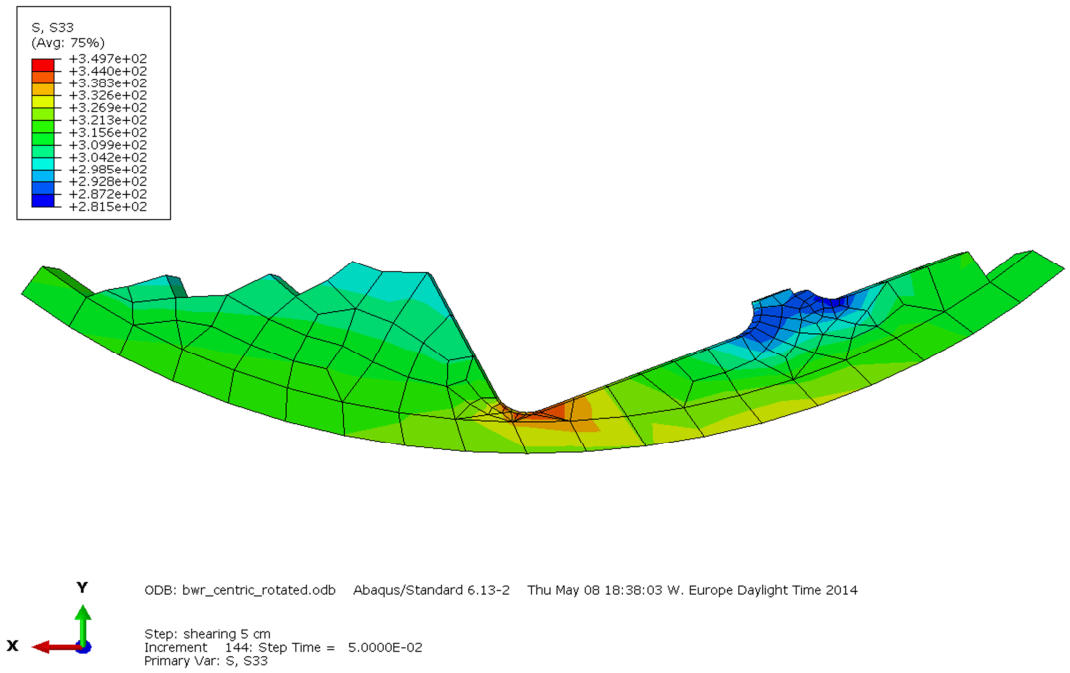

Figure 3-9. The stress in the axial direction (S33) for the model bwr_centric_rotated (magnified as compared to Fig. 3-8).

As shown in Fig. 3-9, the maximum axial stress is located at an inner surface adjacent to the channel tubes (and not located at the outer surface of the insert as in the original analysis). To check this stress more magnification is needed and this is presented in Fig. 3-10 and Fig. 3-11 (with 0% averaging, i.e. no averaging between elements that are connected to each other).

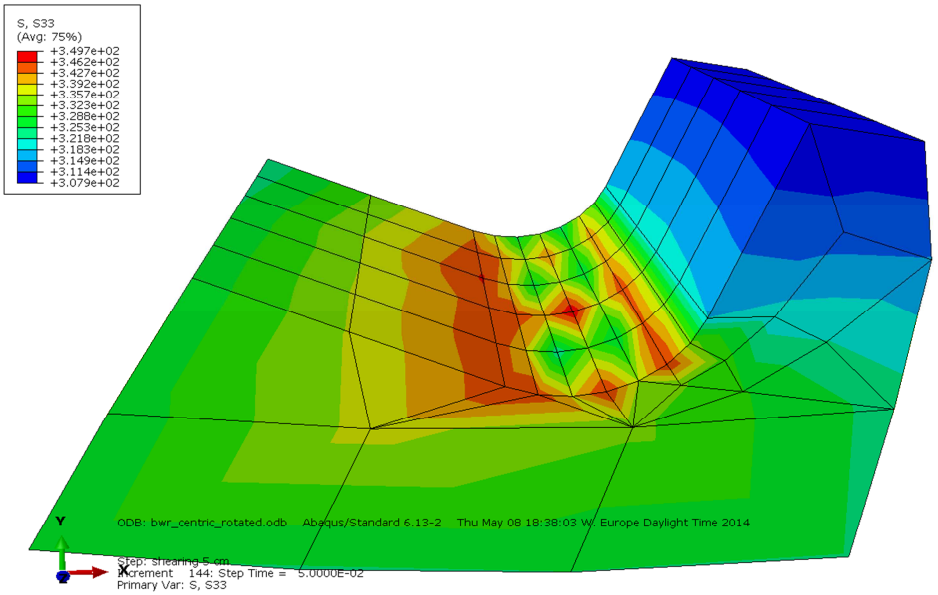

Figure 3-10. The stress in the axial direction (S33) for the model bwr_centric_rotated (magnified as compared to Fig. 3-9).

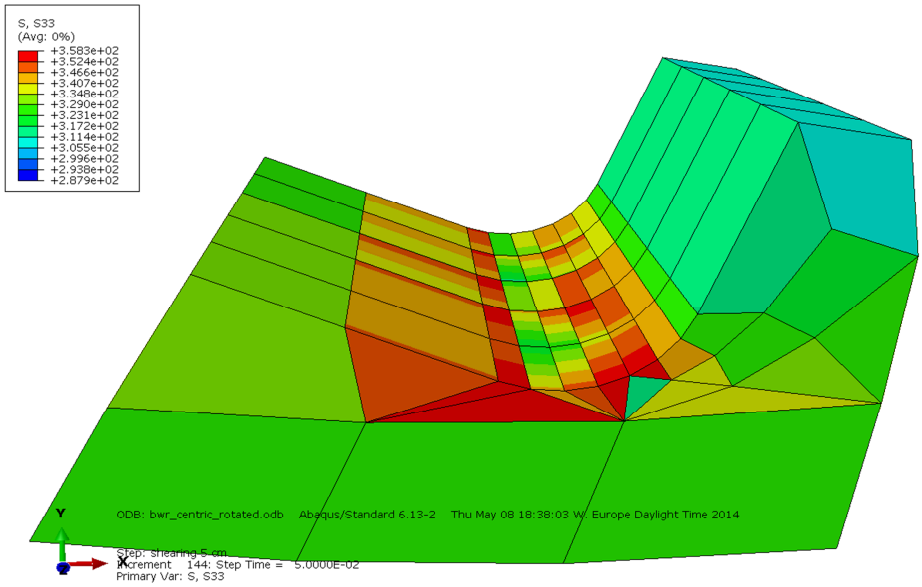

Figure 3-11. The stress in the axial direction (S33) for the model bwr_centric_rotated (magnified as compared to Fig. 3-9 and with 0% averaging between elements).

Examining Fig. 3-10 to 3-11 indicates that the reason for the maximum axial stress to be located at an inner surface adjacent to the channel tubes could be that the elements acts too stiff in this region. This could be a combination of oscillating contact stresses from the channel tubes or/and that the wedge elements behaves poorly (also, there is a need for a mesh refinement in this region). To check this behaviour, the axial stress is plotted along a path in Fig. 3-12.

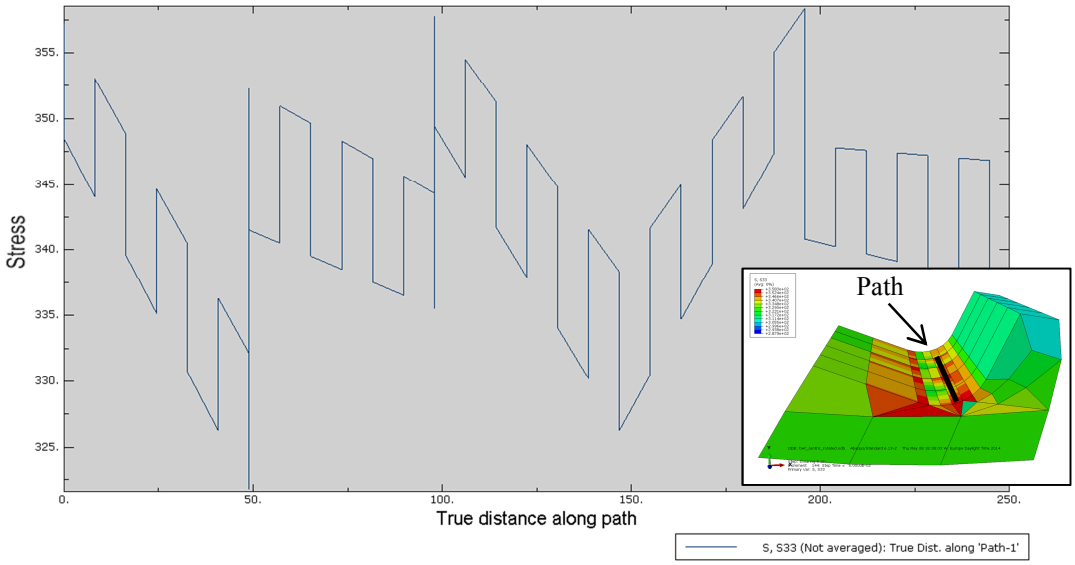

Figure 3-12. The stress in the axial direction (S33), along a given path, for the model model6g_normal_quarter_2050ca3 using 0% averaging between elements (the used path is given as a black line).

The path plot above is shown without averaging and it is obvious that the elements behave poorly in this region. Going along the path one gets both a decrease in axial stress (down to ~320 MPa) and also an increase in axial stress (up to ~360 MPa). A more correct behaviour would be a smooth transition of the stresses and the given maximum axial stress (349.7 MPa) overestimate the stress at the surface of the insert. However, since almost all elements in this region are wedge elements it is quite hard to estimate the error using path plots in different directions.

In a damage tolerance analysis, all the locations with high stresses/strains are probably of minor importance because all the neighbouring elements have consistently significantly lower stresses/strains.

The section where the maximum tensile stresses are located in the original analysis (see Sect. 2.2) are also the most relevant section for this model. Even though the stresses are different in this section (between the two models), 333.3 MPa compared to 349.7 MPa (this stress should be lower according to the discussion above), we believe that the original damage tolerance analysis should be valid and relevant also for this model.

4 RESULTS FROM THE REVISED GLOBAL MODEL (BWR_EXCENTRIC_HALF)

The revised global model bwr_excentric_half is an idealization using a half model, where the steel tube cassette is shifted towards the surface of the insert (i.e. a decreased edge distance as given in Fig. 1-1), but the insert are not rotated. As given in section 1, the revised global model assumes that the channel tubes are not tied to the insert and therefore the contact problem between channel tubes and the insert is now part of the analysis. Also, the support plates are modelled separately from the insert. More details of the revised model are given in [6].

For this model the maximum principal stress is equal to 856.2 MPa and the maximum stress in the axial direction of the insert, S33, is equal to 854.4 MPa (see Fig. 4-1). This shows that there are higher stresses in some areas for this model (compared to the original model).

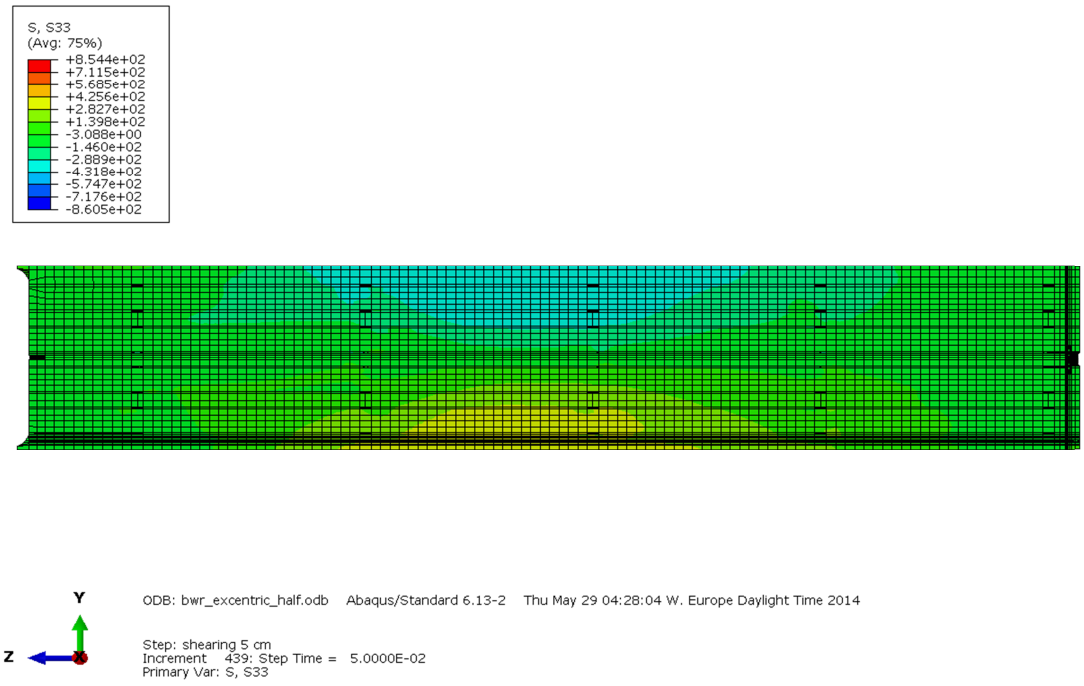

Figure 4-1. The maximum stress in the axial direction (S33) for the model bwr_excentric_half (plot of the entire insert).

The stresses in the section where the maximum tensile stresses were located in the original analysis (see Sect. 2.2) are not higher for this model. The maximum principal stress is equal to 332.9 MPa and the maximum stress in the axial direction of the insert, S33, is equal to 332.3 MPa (see Fig. 4-2). This means that the axial stresses are the most significant in this section, but that there are other areas of the insert that receives significantly higher tensile stresses.

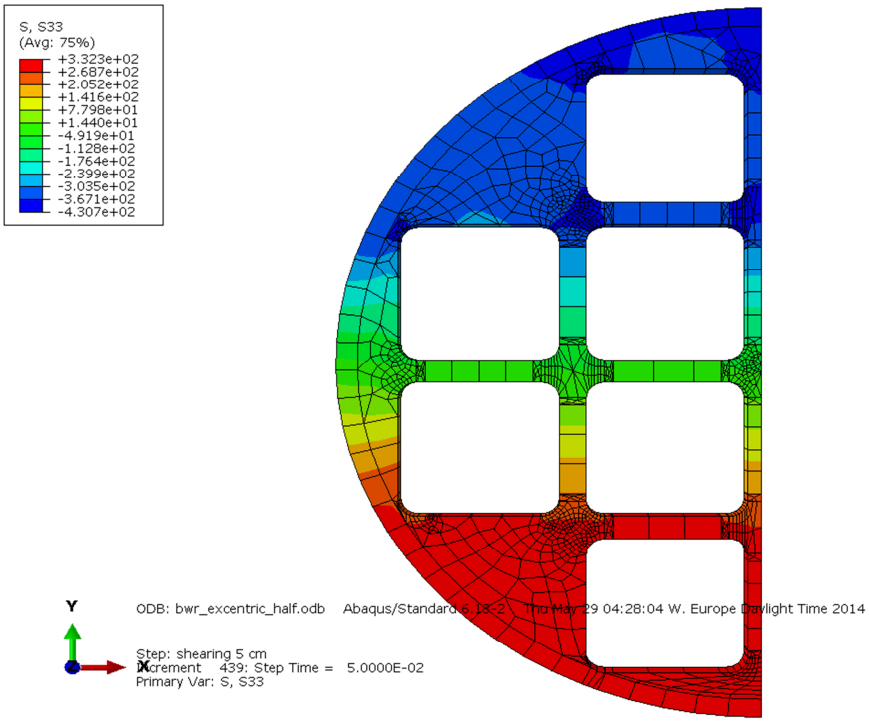

Figure 4-2. The stress in the axial direction (S33) for the model bwr_excentric_half (at the section where the maximum tensile stresses were located in the original analysis).

We start by looking at the base of the insert, where there is a local area of higher tensile stresses, with a maximum principal stress equal to 259.6 MPa (see Fig. 4-3).

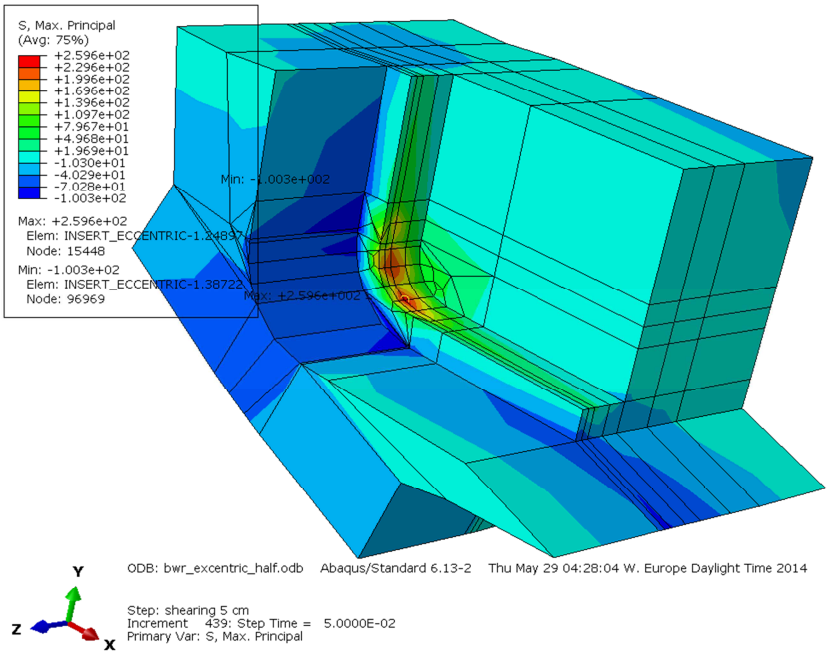

Figure 4-3. The maximum principal stress for the model bwr_excentric_half (at the base of the insert).

The largest stress distribution through the thickness (at the base of the insert), is then compared with the stresses given from the original damage tolerance analysis. This comparison is shown in Fig. 4-4.

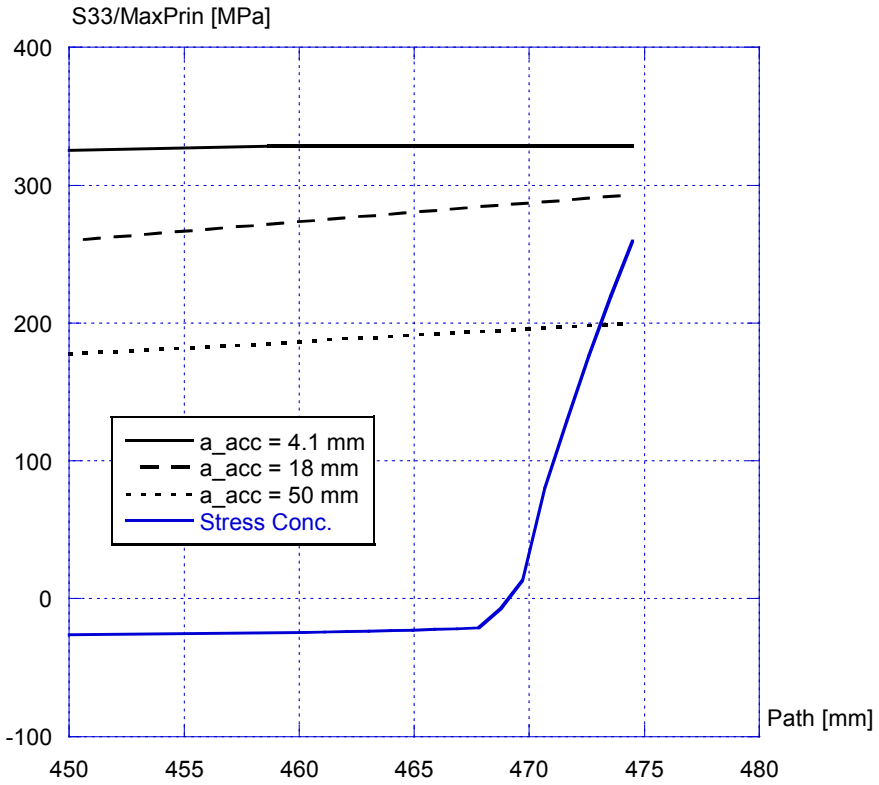

Figure 4-4. Comparison with the largest stress distribution at the base of the insert using different stress distributions (acceptable defect sizes from the original damage tolerance analysis are also given as a function of stresses).

In a damage tolerance analysis, this stress concentration (see Fig. 4-4) is of no major importance because the neighbouring elements have significantly lower stresses.

At the top of the insert there is also a local peak stress of 102.8 MPa (maximum principal stress), see Fig. 4-5.

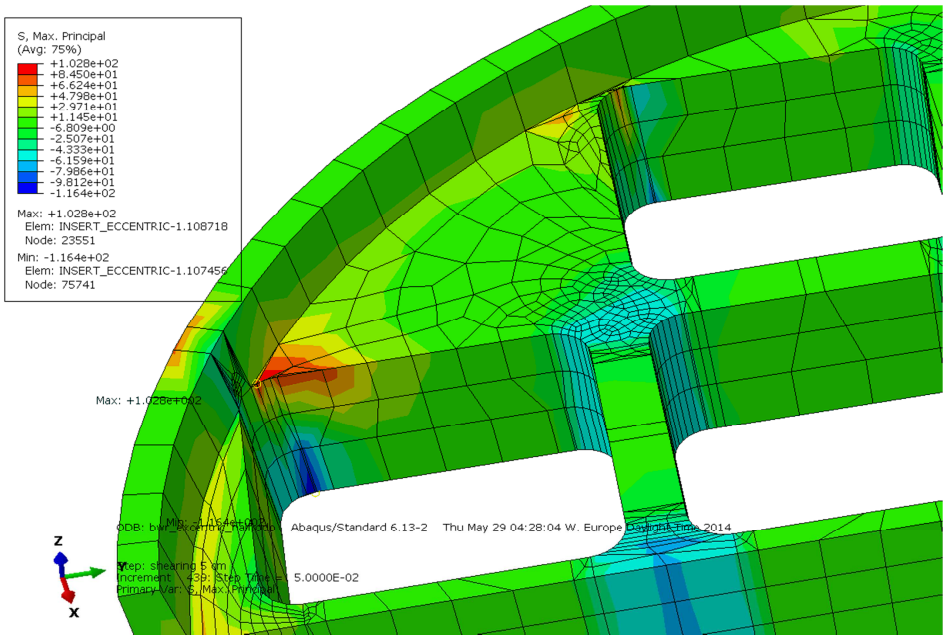

Figure 4-5. The maximum principal stress for the model bwr_excentric_half (at the top of the insert).

As for the base of the insert, in a damage tolerance analysis, this stress concentration is of no major importance because the neighbouring elements have significantly lower stresses (see Fig. 4-6). This means that the locally higher stresses in both the base and top of the insert are without significance for the damage tolerance analysis.

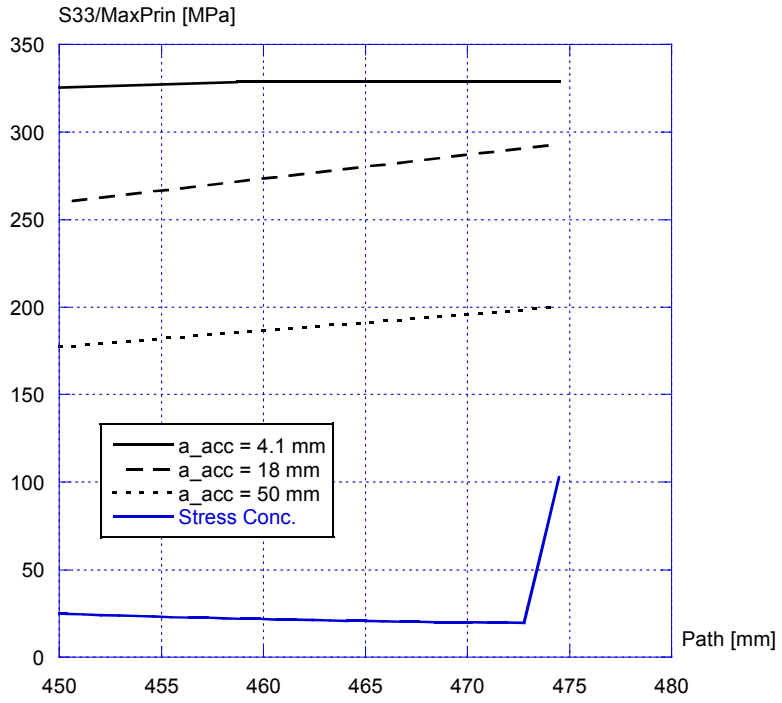

Figure 4-6. Comparison with the largest stress distribution at the top of the insert using different stress distributions (acceptable defect sizes from the original damage tolerance analysis are also given as a function of stresses).

If one removes the base and top part of the insert, the remaining part of the insert has a maximum principal stress equal to 856.2 MPa. This means that we still have a local tensile stress that is significantly higher than in the original section as given in Fig. 4-2. Zooming into the area with high stresses, one can see that this high stress is concentrated to a number of elements adjacent to the now-modelled support plates that hold together the channel tubes (see Fig. 4-7).

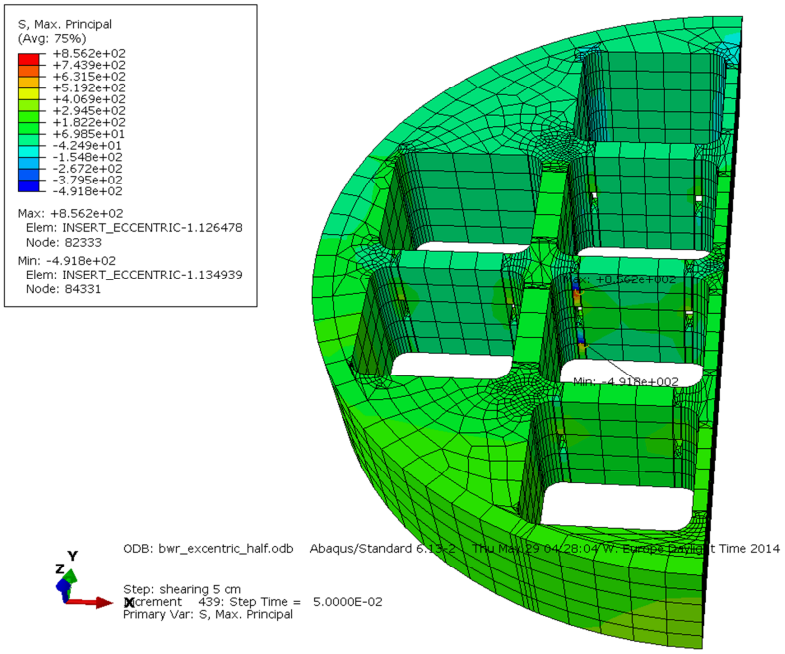

Figure 4-7. The maximum principal stress for the model bwr_excentric_half (location with a local stress equal to 856.2 MPa).

As seen in the plot above, these elements seems to behave incorrect, therefore we look more closely at the point with high stresses (see Fig. 4-8).

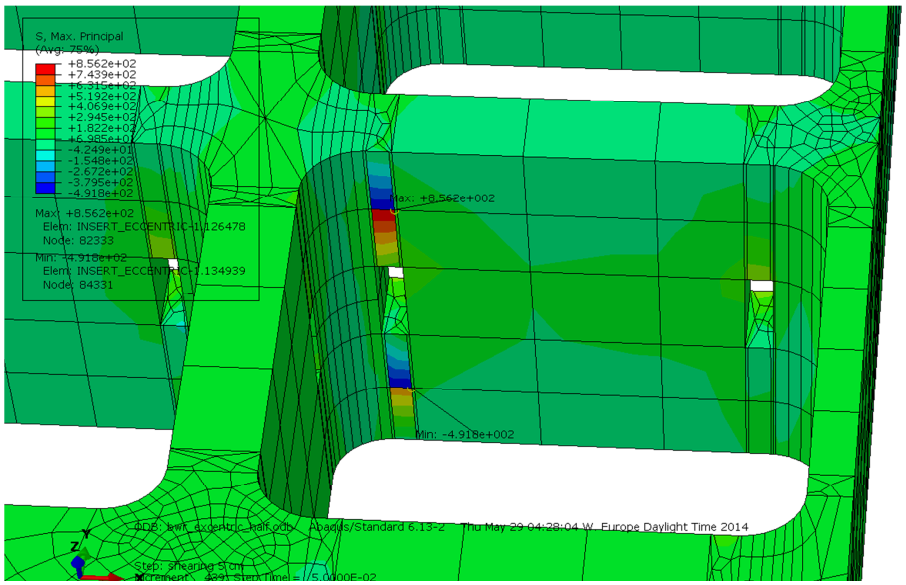

Figure 4-8. The maximum principal stress for the model bwr_excentric_half (location with a local stress equal to 856.2 MPa). The support plates are not part of the insert and are therefore not shown in this figure (i.e. the holes represent the positions of the support plates).

Examining Fig. 4-8 shows that the reason for the high stresses is that the wedge elements behave poorly and are too stiff in this region. To show the poor behaviour more clearly, the maximum principal stress is plotted along a path in Fig. 4-9 (including the two elements with poor behaviour).

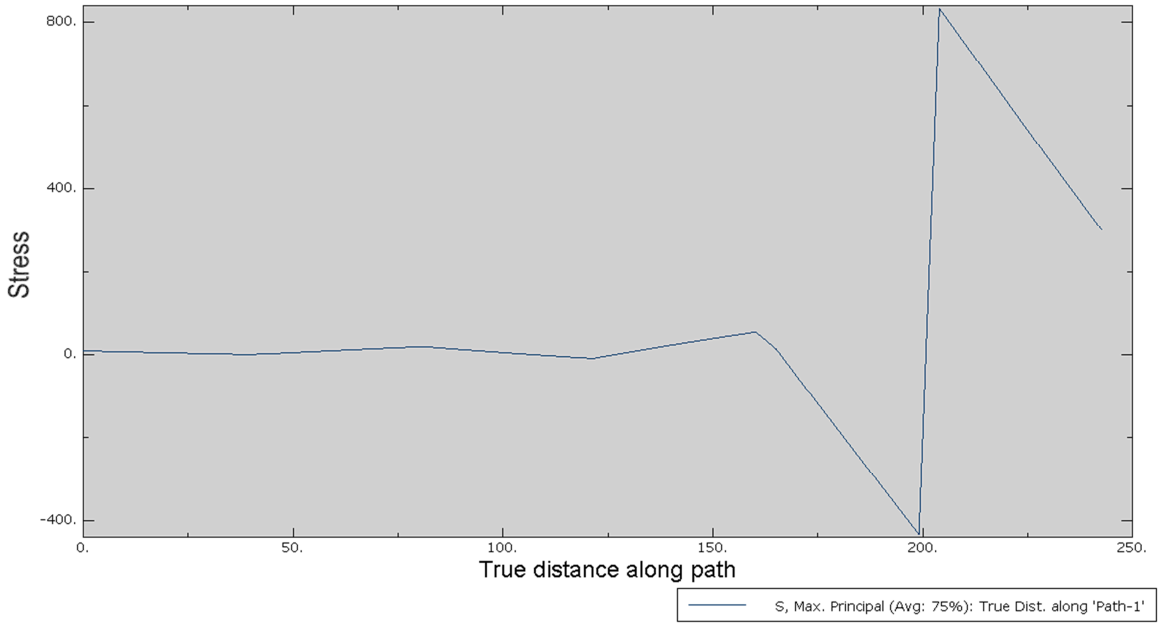

Fig. 4-9. The maximum principal stress for the model bwr_excentric_half (along a path at the location with a local stress equal to 856.2 MPa).

What is clearly show in Fig. 4-9 is that the maximum principal stress goes from approximately -400 MPa to +800 MPa at the same point in the model and the results from these elements are incorrect and should therefore be disregarded. Also, all the surrounding elements have very low stresses (less than 100 MPa) which are reasonably in this part of the model.

If we check the effective plastic strain there is small region (where the insert is adjacent to the channel tubes, see Fig. 4-10) with strains equal to 2.9% (using 0% averaging between elements). Here, all the plastic strain is concentrated to a layer of elements and all neighbouring elements have lower strains (another plot is given in Fig. 4-11). These elements are too stiff and should not be used in a damage tolerance analysis.

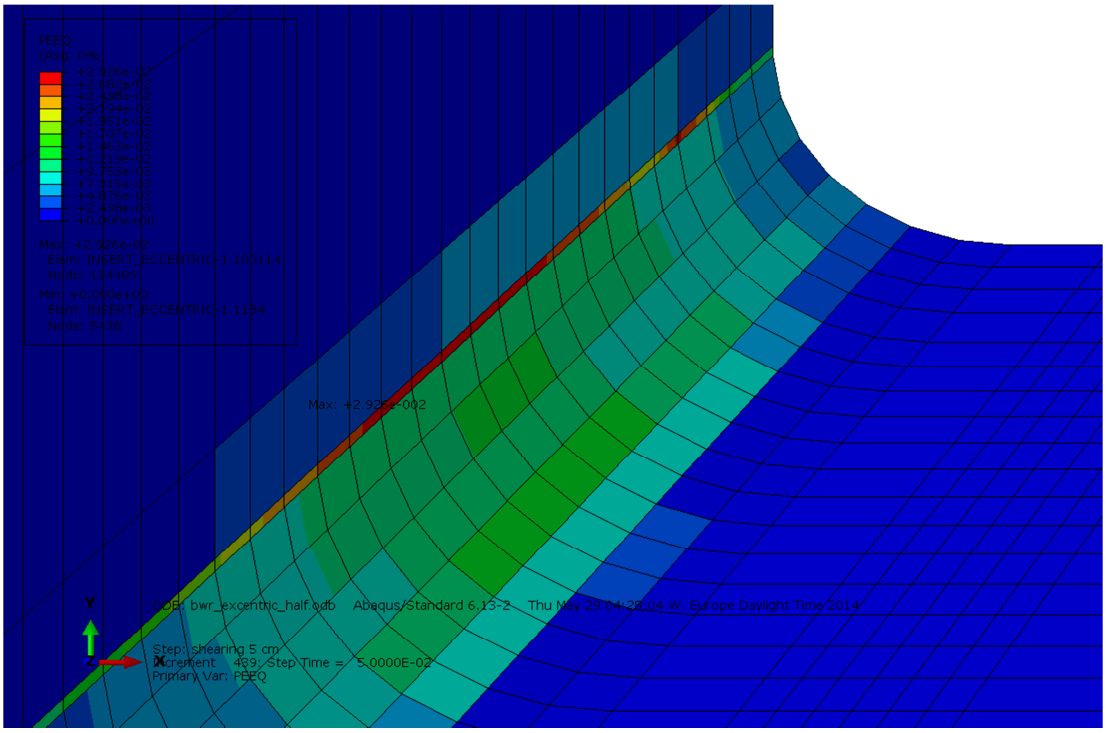

Figure 4-10. The effective plastic strain for the model bwr_excentric_half using 0% averaging between elements (at a location where the insert is adjacent to the channel tubes).

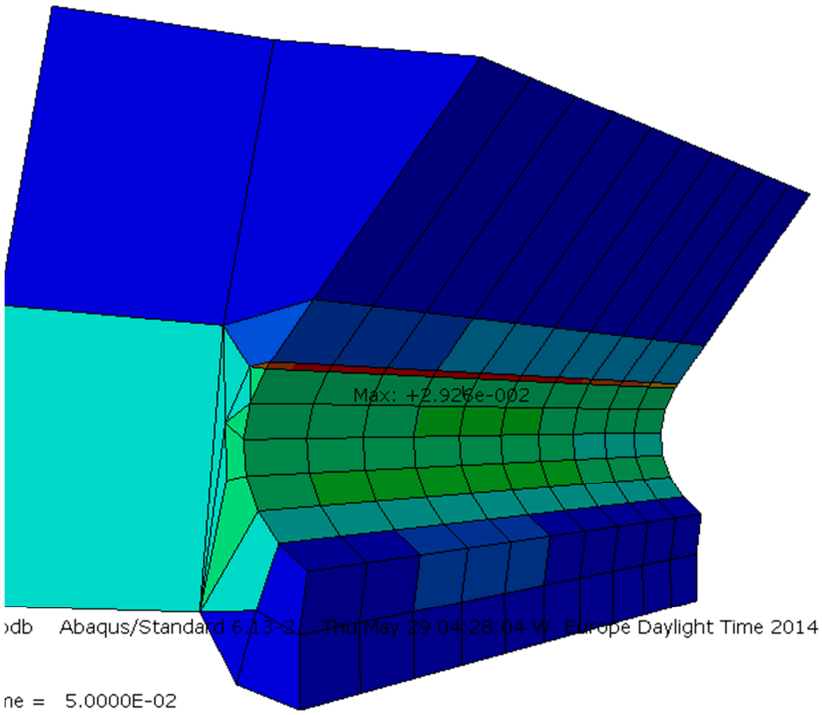

Figure 4-11. The effective plastic strain for the model bwr_excentric_half using 0% averaging between elements (at a location where the insert is adjacent to the channel tubes). The poorly behaved wedge elements are shown in red.

In a damage tolerance analysis, all the locations with high stresses/strains are of minor importance because all the neighbouring elements have consistently significantly lower stresses/strains.

Finally, the section where the maximum tensile stresses are located in the original analysis (see Sect. 2.2) are therefore the most relevant section for this model. Since the stresses are almost equal in this section (between the two models), 333.3 MPa compared to 332.9 MPa, the original damage tolerance analysis should be valid and relevant also for this model.

5 RESULTS FROM THE REVISED GLOBAL MODEL (BWR_EXCENTRIC_ROTATED)

The revised global model bwr_excentric_rotated is an idealization using a full model, where the steel tube cassette is shifted towards the surface of the insert (i.e. a decreased edge distance as given in Fig. 1-1) and the insert is rotated to have a small distance between the channel corner and insert outer radius (at the position with large axial stresses). As given in section 1, the revised global model assumes that the channel tubes are not tied to the insert and therefore the contact problem between channel tubes and the insert is now part of the analysis. Also, the support plates are modelled separately from the insert. More details of the revised model are given in [6].

For this model the maximum principal stress is equal to 532.3 MPa and the maximum stress in the axial direction of the insert, S33, is equal to 516.5 MPa (see Fig. 5-1). This shows that there are higher stresses in some areas for this model (compared to the original model).

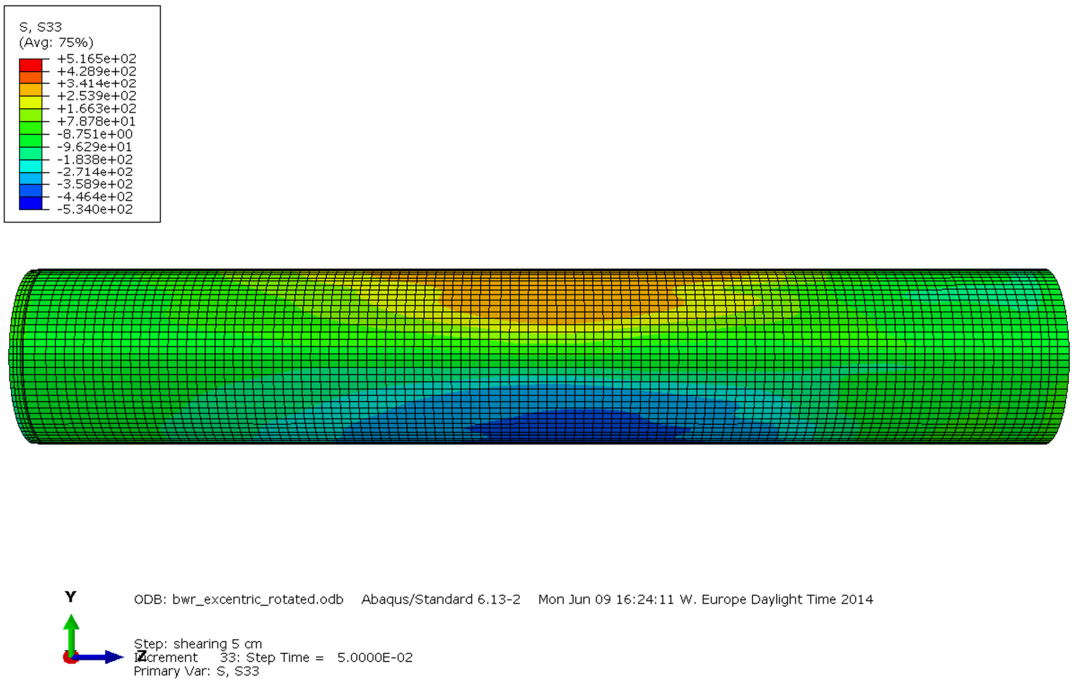

Figure 5-1. The maximum stress in the axial direction (S33) for the model bwr_excentric_rotated (plot of the entire insert).

The stresses in the section where the maximum tensile stresses were located in the original analysis (see Sect. 2.2) are not higher for this model (except for one element, which is discussed later in this section). Both the maximum principal stress and the maximum stress in the axial direction of the insert, S33, are then equal to 339.0 MPa. This means that the axial stresses are the most significant in this section, but that there are other regions of the insert that receives significantly higher tensile stresses.

We start by looking at the base of the insert, where there is a local region of higher tensile stresses, with a maximum principal stress equal to 229.3 MPa (see Fig. 5-2).

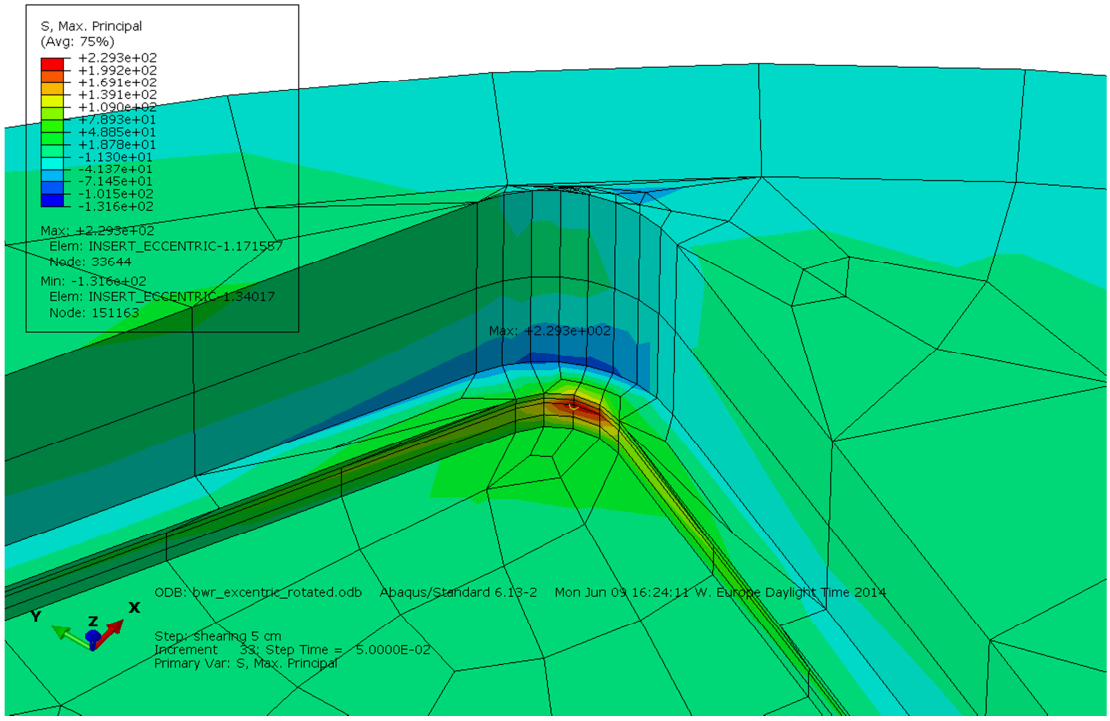

Figure 5-2. The maximum principal stress for the model bwr_excentric_rotated (at the base of the insert).

The largest stress distribution through the thickness (at the base of the insert), is then compared with the stresses given from the original damage tolerance analysis. This comparison is shown in Fig. 5-3.

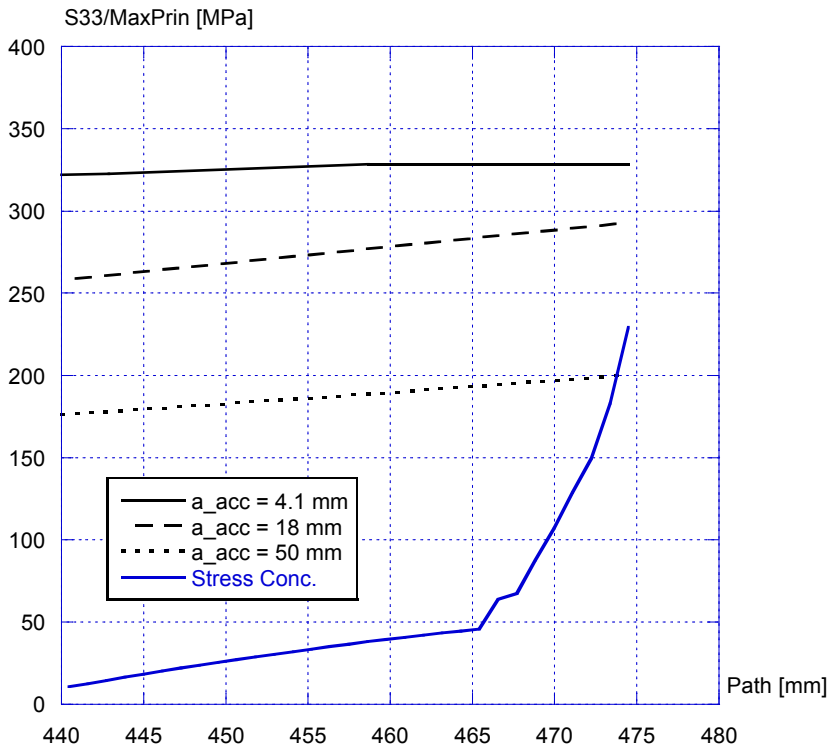

Figure 5-3. Comparison with the largest stress distribution at the base of the insert using different stress distributions (acceptable defect sizes from the original damage tolerance analysis are also given as a function of stresses).

In a damage tolerance analysis, this stress concentration (see Fig. 5-3) is of no major importance because the neighbouring elements have significantly lower stresses.

At the top of the insert there is also a local peak stress of 165.3 MPa (maximum principal stress), see Fig. 5-4.

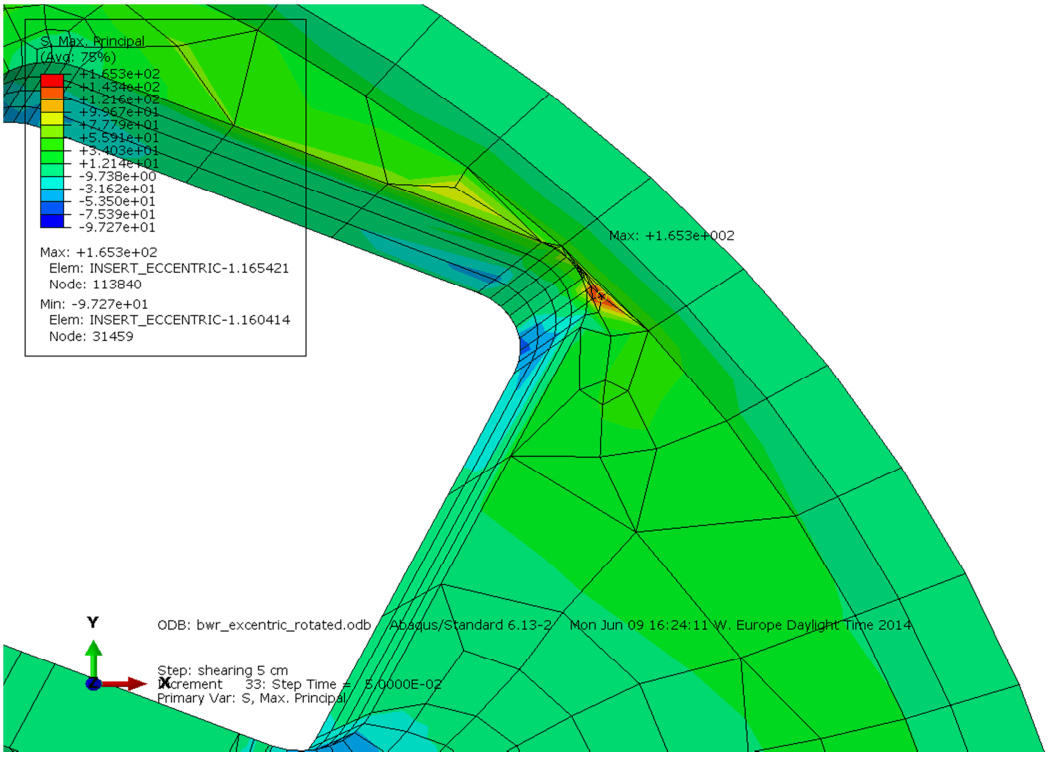

Figure 5-4. The maximum principal stress for the model bwr_excentric_rotated (at the top of the insert).

As for the top of the insert, in a damage tolerance analysis, this stress concentration is of no major importance because the neighbouring elements have significantly lower stresses (see Fig. 5-5). This means that the locally higher stresses in both the base and top of the insert are without significance for the damage tolerance analysis.

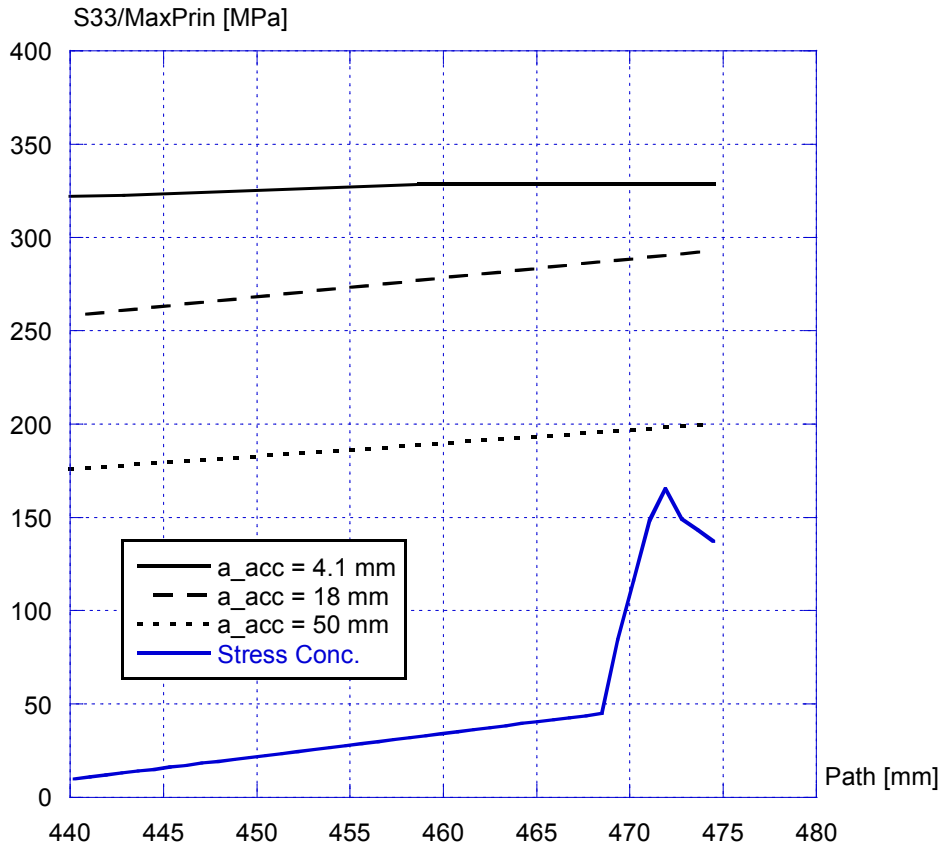

Figure 5-5. Comparison with the largest stress distribution at the top of the insert using different stress distributions (acceptable defect sizes from the original damage tolerance analysis are also given as a function of stresses).

If one removes the base and top part of the insert, the remaining part of the insert has a maximum principal stress equal to 532.3 MPa. This means that we still have a local tensile stress that is significantly higher than in the original section. Zooming into the area with high stresses, one can see that this high stress is concentrated to a number of elements adjacent to the now-modelled support plates that hold together the channel tubes (see Fig. 5-6).

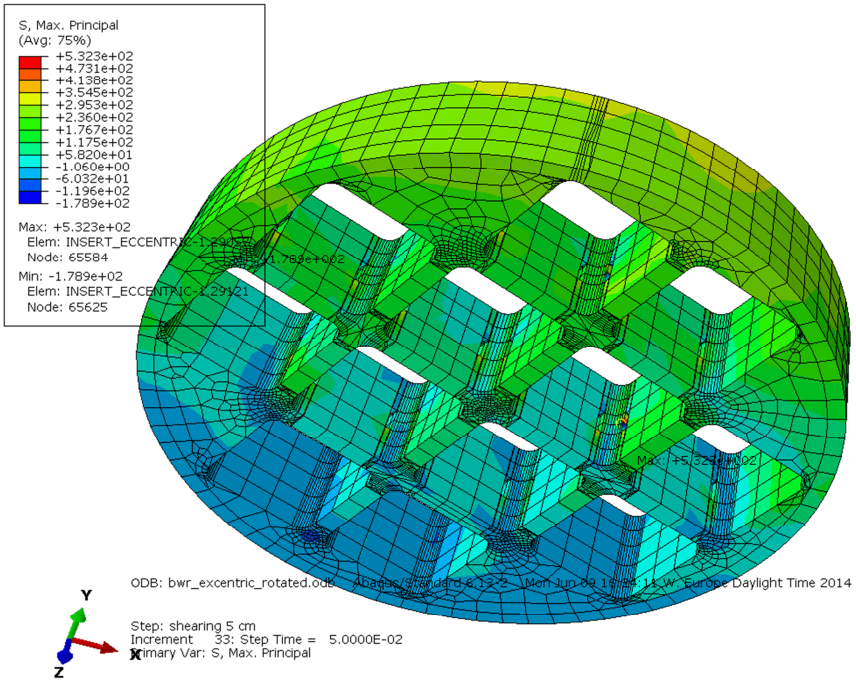

Figure 5-6. The maximum principal stress for the model bwr_excentric_rotated (location with a local stress equal to 532.3 MPa).

As seen in the plot above, these elements seems to behave somewhat incorrect, therefore we look more closely at the point with high stresses (see Fig. 5-7).

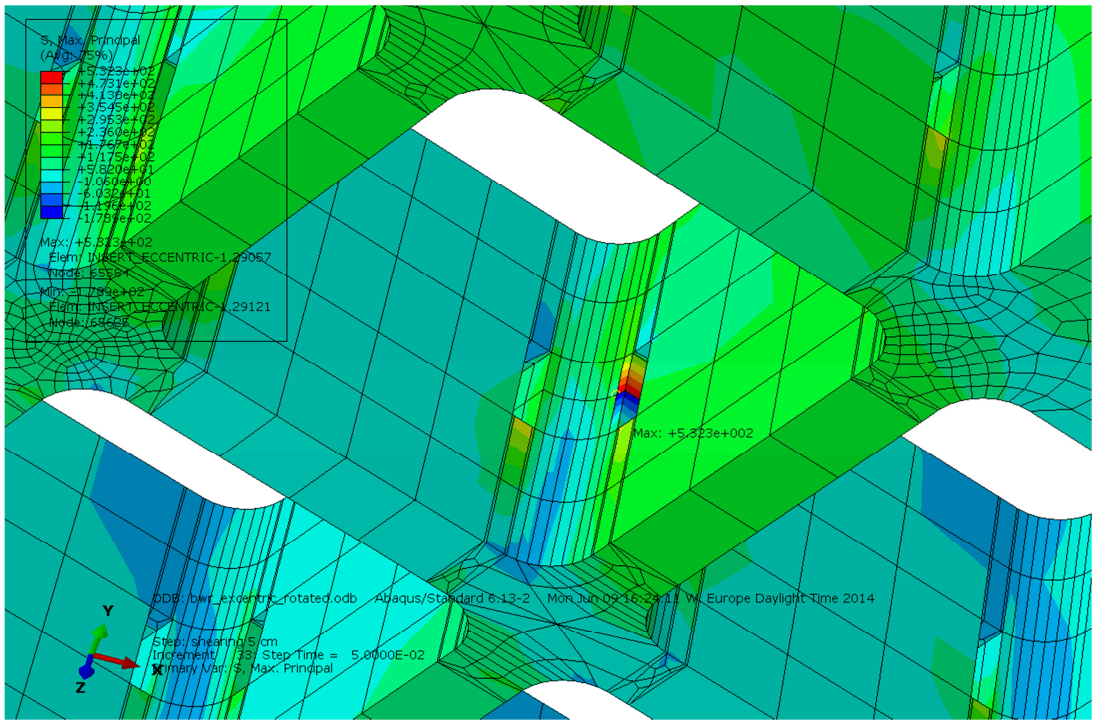

Figure 5-7. The maximum principal stress for the model bwr_excentric_rotated (location with a local stress equal to 532.3 MPa).

Examining Fig. 5-7 shows that the reason for the high stresses is that the elements behave poorly and are too stiff in this region. To show the poor behaviour more clearly, the maximum principal stress is plotted along a path in Fig. 5-8 (including the two elements with poor behaviour).

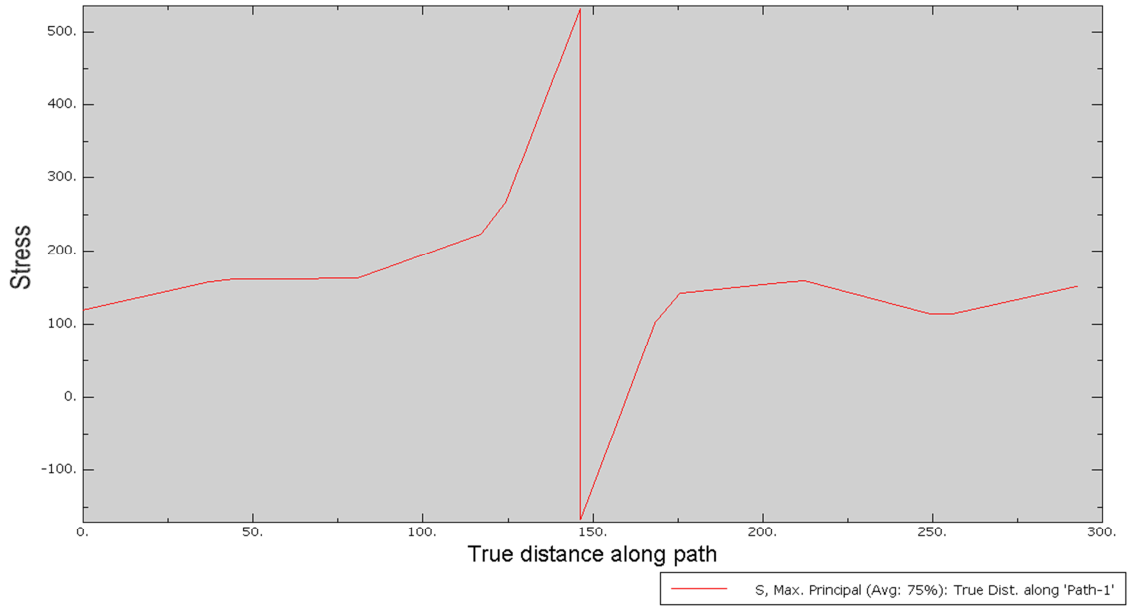

Fig. 5-8. The maximum principal stress for the model bwr_excentric_rotated (along a path at the location with a local stress equal to 532.3 MPa).

What is clearly show in Fig. 5-8 is that the maximum principal stress goes from approximately -150 MPa to +530 MPa at the same point in the model and the results from these elements are incorrect and should therefore be disregarded. Also, all the surrounding elements have lower stresses (less than 200 MPa) which are reasonably in this part of the model.

If we check the effective plastic strain there is small region (where the insert is adjacent to the channel tubes and one of the support plates, see Fig. 5-9) with strains equal to 2.4% (using 0% averaging between elements). Here, all the plastic strain is concentrated to one element and all neighbouring elements have lower strains. This element is too stiff and should not be used in a damage tolerance analysis (another plot is given in Fig. 5-10).

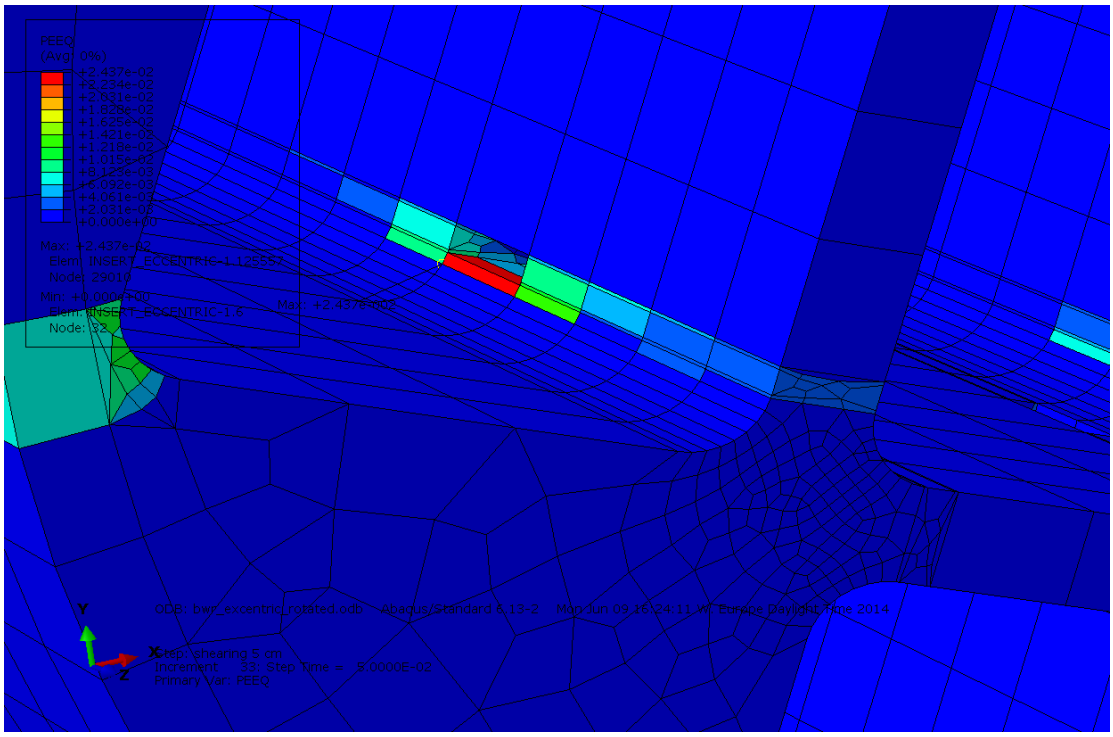

Figure 5-9. The effective plastic strain for the model bwr_excentric_rotated using 0% averaging between elements (at a location where the insert is adjacent to the channel tubes and one of the support plates).

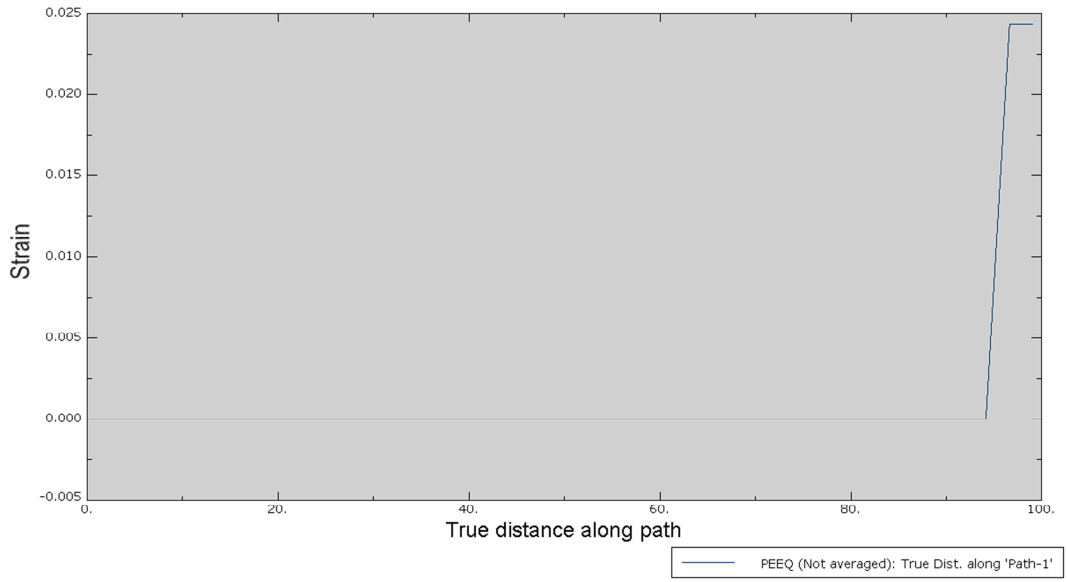

Figure 5-10. The effective plastic strain for the model bwr_excentric_rotated using 0% averaging between elements (along a path at the location with a local plastic strain equal to 2.4 %).

The effective plastic strain along a path, as given in Fig. 5-10, clearly shows that the element behaves incorrectly. All the other elements along the path (possible growth direction of a postulated crack) have no plastic strain.

In a damage tolerance analysis, all the locations with high stresses/strains are of minor importance because all the neighbouring elements have consistently significantly lower stresses/strains.

Finally, the section where the maximum tensile stresses are located in the original analysis (see Sect. 2.2) are therefore the most relevant section for this model also (see Fig. 5-11). In this section (for this model) we identify two regions of interest. First is the expected position where we have an axial stress equal to 339.0 MPa, but there is also a position with higher axial stress equal to 379.9 MPa.

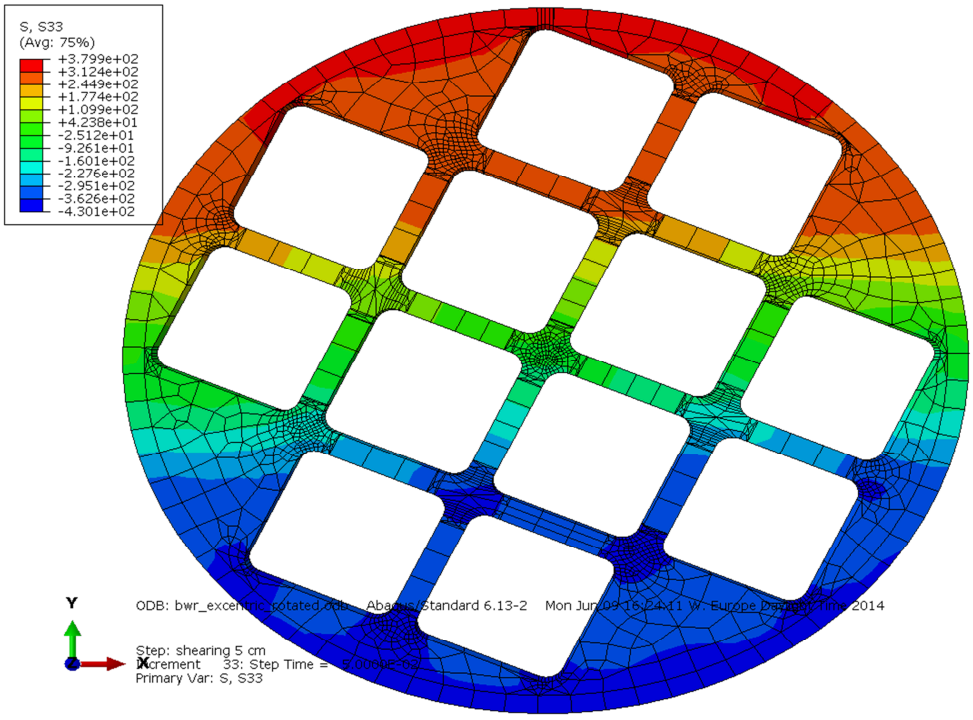

Figure 5-11. The stress in the axial direction (S33) for the model bwr_excentric_rotated (at the section where the maximum tensile stresses were located in the original analysis).

First we investigate the position that has slightly higher stress in the axial direction (S33 = 379.9 MPa) and find that it is located on the inside close to one of the channel tubes (see Fig. 5-12).

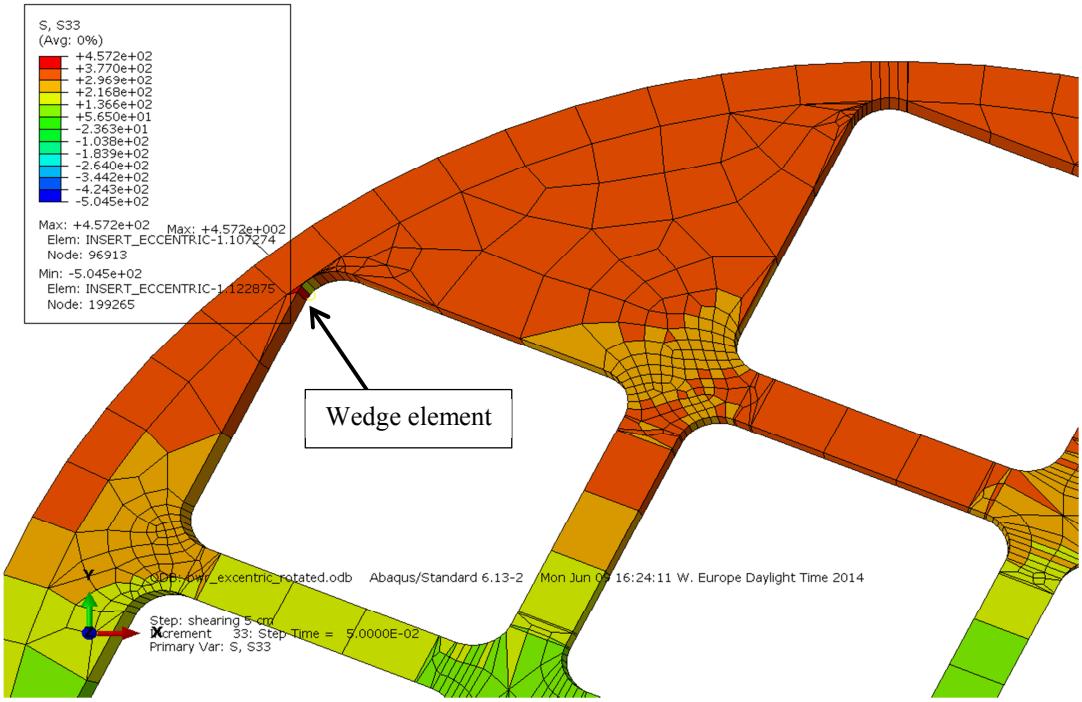

Figure 5-12. The stress in the axial direction (S33) for the model bwr_excentric_rotated (at a position on the inside close to one of the channel tubes).

The plot above is without averaging and we then obtained S33 = 457.2 MPa. One can see that this stress is present in one wedge element only and that the element behaves poorly (it is too stiff) as compared to all neighbouring elements. The stresses from this element should not be used in a damage tolerance analysis (compare the stresses given in Fig. 2-5).

We now investigate the expected position where we have an axial stress equal to 339.0 MPa (see Fig. 5-13).

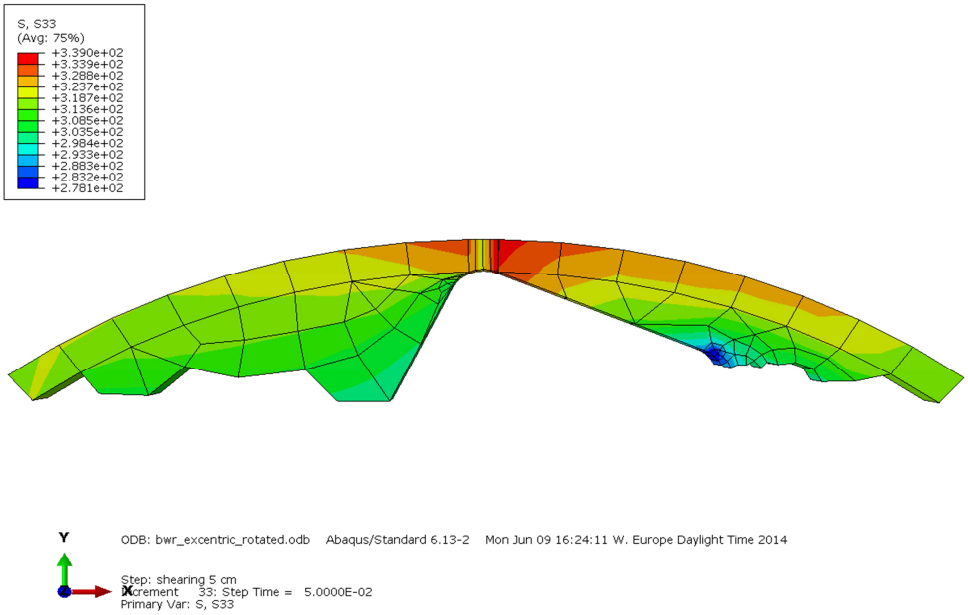

Figure 5-13. The stress in the axial direction (S33) for the model bwr_excentric_rotated (at the expected position on the surface of the insert).

As shown in Fig. 5-13, the maximum axial stress is located between the channel tubes and the outer surface of the insert (as in the original analysis). However, the maximum stress is not symmetric in this region and therefore we also plot this with 0% averaging between elements (see Fig. 5-14).

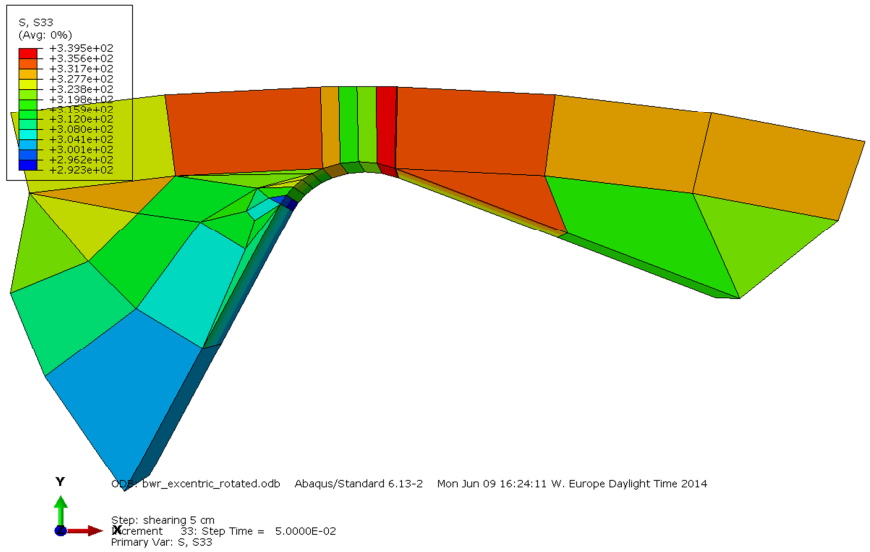

Figure 5-14. The stress in the axial direction (S33) for the model bwr_excentric_rotated (at the expected position on the surface of the insert, with 0% averaging between elements).

As shown in Fig. 5-14, the axial stress varies at the location with the smallest distance between the channel tubes and the outside of the insert. The reason for this could be that there is a very thin element to the right of the element with largest axial stresses (there is also a need for a mesh refinement in this region). To check this behaviour, the axial stress is plotted along a path in Fig. 5-15.

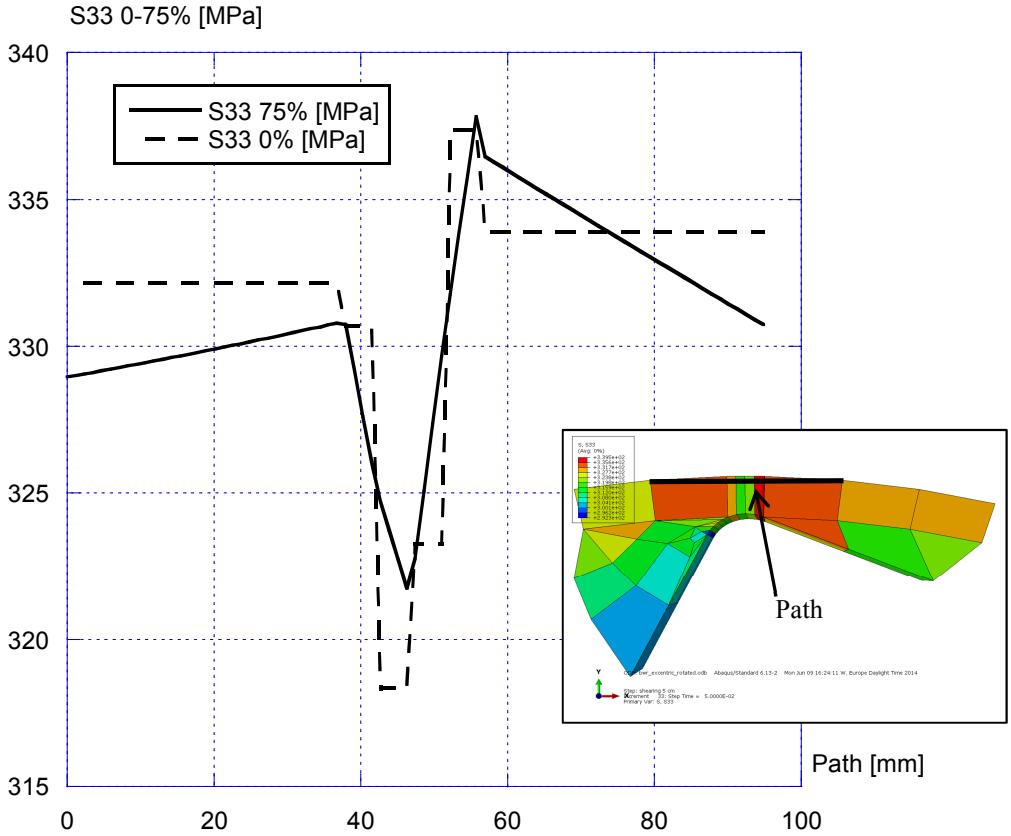

Figure 5-15. A path plot of the stress in the axial direction (S33) with 0% or 75% averaging between elements (the used path is given as a black line).

The path plot above is shown with and without averaging and it is obvious that the elements behave poorly in this region. Going along the path one gets both a decrease in axial stress (down to ~320 MPa) and also an increase in axial stress (up to ~340 MPa). A more correct behaviour would be a smooth transition of the stresses (somewhere between ~330 MPa to ~335 MPa) and the given maximum axial stress (339.0 MPa) slightly overestimate the stress at the surface of the insert.

Finally, we choose to look at the effective plastic strain at the same section (see Fig. 5-16). The maximum plastic strain is 0.33% and it is located where the distance between the channel tubes and the outside of the insert is smallest.

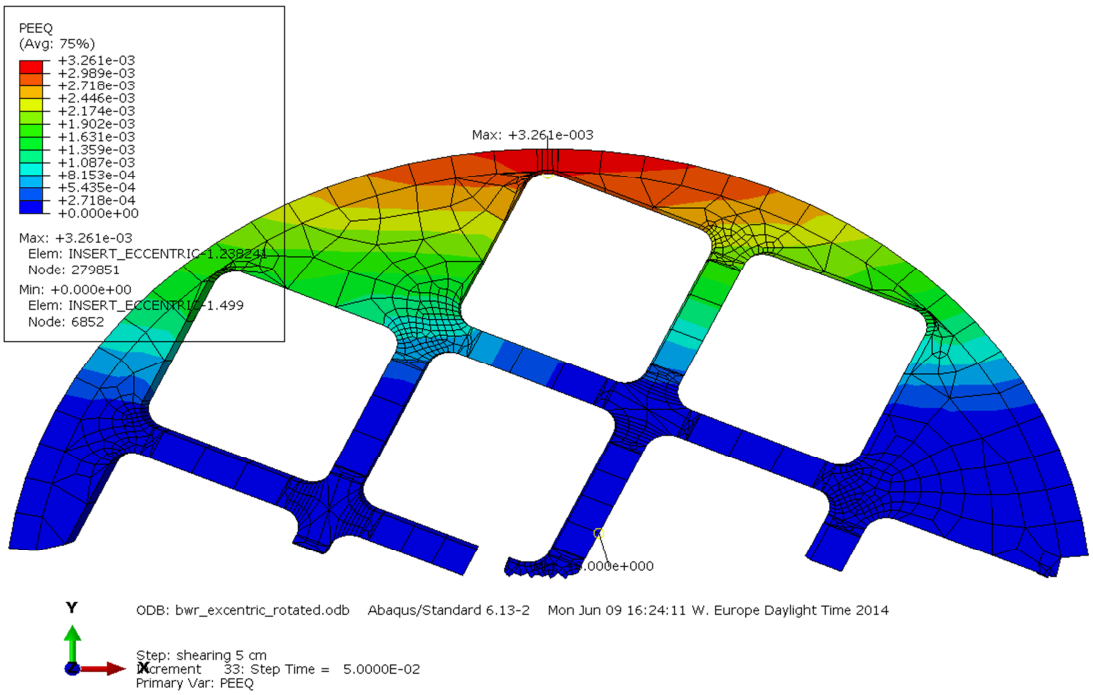

Figure 5-16. The effective plastic strain for the model bwr_excentric_rotated (at the section where the maximum tensile stresses were located in the original analysis).

In a damage tolerance analysis, all the locations with high stresses/strains are probably of minor importance because all the neighbouring elements have consistently significantly lower stresses/strains.

The section where the maximum tensile stresses are located in the original analysis (see Sect. 2.2) are also the most relevant section for this model. Since the stresses are almost equal in this section (between the two models), 333.3 MPa compared to 339.0 MPa (this stress should be somewhat lower according to the discussion above), the original damage tolerance analysis should be valid and relevant also for this model.

6 SUMMARY AND CONCLUSIONS

In this report, a comparison is made between the original model of the BWR insert (using a simplified idealization of the geometry) and a more advanced model where the channel tubes are not tied to the insert and the support plates are modelled separately from the insert. Also, the impact of manufacturing tolerances is evaluated, where the steel tube cassette is shifted so that it is closer to the outside of the insert (i.e. a decreased edge distance).

The comparison shows that all the new models have locally higher stresses compared to the original model. The reason for these high stresses is mainly dependent on the element meshes, which are not designed to be used in a damage tolerance analysis. For example, many stress concentrations is directly related to the use of wedge elements. In all cases, disregarding the elements that behaves poorly significantly reduces the locally higher tensile stresses. There are also regions with slightly elevated stress concentrations, but they are of minor importance because the neighbouring elements have significantly lower stresses.

Both the original model and all the new models have axial stresses of the same magnitude in the most important region for the damage tolerance analysis. This shows that it is not necessary to perform a completely renewed damage tolerance analysis at more positions in the insert or at the location with the smallest distance between the channel tubes and the outside of the insert.

7 REFERENCES

[1] RAIKO, H., SANDSTRÖM, R., RYDÉN, H. and JOHANSSON, M., (2010-04), "Design analysis report for the canister", SKB Technical Report TR-10-28, Swedish Nuclear Fuel and Waste Management Co.

[2] BRICKSTAD, B., (2012-09-11), "Begäran om komplettering av ansökan om slutförvaring av använt kärnbränsle och kärnavfall - kapselns mekaniska integritet", SSM2011-2426, Strålsäkerhetsmyndigheten.

[3] HERNELIND, J., (2014-02-13), "Detailed models for PWR- and BWR-canisters for Earthquake induced rock shearing", SKB Public Report, DocID 1415152, Ver. 2.0, Swedish Nuclear Fuel and Waste Management Co.

[4] HERNELIND, J., (2010-08), "Modelling and analysis of canister and buffer for earthquake induced rock shear and glacial load", SKB Technical Report TR-10-34, Swedish Nuclear Fuel and Waste Management Co.

[5] —, (2014-03-12), "Protokoll från avstämningsmöte SSM-SKB angående kapselns mekaniska integritet, tillverkningsaspekter samt kontroll och provning", Dok.nr: SSM2011-1137-58, Strålsäkerhetsmyndigheten.

[6] HERNELIND, J., (2014-10-15), "Detailed models for BWR-canisters for Earthquake induced rock shearing", SKB Öppen Report, DocID 1439722, Ver. 1.0, Swedish Nuclear Fuel and Waste Management Co.

[7] DILLSTRÖM, P. and BOLINDER, T., (2010-10), "Damage tolerance analysis of canister inserts for spent nuclear fuel in the case of an earthquake induced rock shear load", SKB Technical Report TR-10-29, Swedish Nuclear Fuel and Waste Management Co.

[8] —, (2013-10), "Design, production and initial state of the canister", SKB Technical Report TR-10-14, Updated 2013-10, Swedish Nuclear Fuel and Waste Management Co.

[9] DILLSTRÖM, P., and W. ZANG., (2004), "User manual ProSACC Version 1.0", DNV Research Report 2004/02, Det Norske Veritas AB, Stockholm, Sweden.

8 TABLE OF REVISIONS

Rev	Reason for change/Pages or chapters	Our reference	Date
0	—	Peter Dillström	2014-10-21
1	The report is revised according to the review comments in SKBDoc 1451903, Ver. 0.5.	Peter Dillström	2014-12-10
2	The report is revised according to the review comments in SKBDoc 1465102, Ver. 0.2.	Peter Dillström	2015-01-29